

UNIVERSITY OF AMSTERDAM

MASTERS THESIS

---

Parameter optimization via an  
evolutionary algorithm of  
reaction-diffusion models describing the  
asymmetric gene expression of the  
sea-anemone *Nematostella vectensis*

---

*Author:*

Nick VAN SANTEN

*Supervisors:*

Jaap Kaandorp

Renske Vroomans

*A thesis submitted in partial fulfilment of the requirements  
for the degree of Master of Science in Computational Science*

*in the*

Computational Science Lab

Informatics Institute

June 2023



# Declaration of Authorship

I, Nick VAN SANTEN, declare that this thesis, entitled ‘Parameter optimization via an evolutionary algorithm of reaction-diffusion models describing the asymmetric gene expression of the sea-anemone *Nematostella vectensis*’ and the work presented in it are my own. I confirm that:

- This work was done wholly or mainly while in candidature for a research degree at the University of Amsterdam.
- Where any part of this thesis has previously been submitted for a degree or any other qualification at this University or any other institution, this has been clearly stated.
- Where I have consulted the published work of others, this is always clearly attributed.
- Where I have quoted from the work of others, the source is always given. With the exception of such quotations, this thesis is entirely my own work.
- I have acknowledged all main sources of help.
- Where the thesis is based on work done by myself jointly with others, I have made clear exactly what was done by others and what I have contributed myself.

Signed:

A handwritten signature in dark ink, appearing to read 'Nick', is written over a horizontal line.

Date: 21 June 2023

*“Simplicity, carried to the extreme, becomes elegance”*

Jon Franklin

UNIVERSITY OF AMSTERDAM

# *Abstract*

Faculty of Science  
Informatics Institute

Master of Science in Computational Science

**Parameter optimization via an evolutionary algorithm of reaction-diffusion  
models describing the asymmetric gene expression of the sea-anemone  
*Nematostella vectensis***

by Nick VAN SANTEN

The bilateral development of an embryo of the sea-anemone *Nematostella vectensis* is studied through a set of models simulating different gene regulatory networks, which describe the interactions between different genes. This thesis will look into sixteen variations of a core gene regulatory network. The core network is a simplified network taken from previous research of the bilateral embryonic development of *Nematostella vectensis* and contains three genes: BMP, Chd, and W. The networks are simulated through reaction-diffusion equations on a mesh surface representing the mesoglea of the embryo.

Many parameters of the sixteen variations are unknown. The parameters of the sixteen networks are optimized for each of the sixteen networks. The optimization of the parameters is achieved by fitting the computed gene expression against observational in-situ data. The fitting of the parameters will be performed by an evolutionary algorithm followed by a local search, implemented by the downhill-simplex method. Knock-down experiments will then be performed to verify the optimized parameters.

The evolutionary algorithm identified eight networks which were able to replicate the observational in-situ data and four other networks which showed asymmetric expression but did not match with the in-situ data. The downhill-simplex method did not improve the fitness of the networks significantly and was therefore not used in the final results.

A qualitative comparison was performed to verify the successful models with knock-down experiments. Several networks, and one network in particular, appeared to match the knock-down experiments. However, a proposed quantitative analysis would need to be performed to actually verify the knock-down results.

## *Acknowledgements*

I want to express my thanks to Jaap Kaandorp and Renske Vroomans for guiding me through this project and the discussions we had. I could not have done this without them. Furthermore, I want to thank Grigory Genikhovich for his continued support with the *Nematostella vectensis* projects and Steven Oud for providing me with the network figures. At last, I want to thank Koen Greuell for his assistance with the data processing.

# Contents

<b>Declaration of Authorship</b>	<b>i</b>
<b>Abstract</b>	<b>iii</b>
<b>Acknowledgements</b>	<b>iv</b>
<b>Contents</b>	<b>v</b>
<b>List of Figures</b>	<b>vii</b>
<b>List of Tables</b>	<b>x</b>
<b>List of Algorithms</b>	<b>xi</b>
<b>Abbreviations</b>	<b>xii</b>
<b>1 Introduction</b>	<b>1</b>
1.1 The model organism <i>Nematostella vectensis</i> . . . . .	1
1.2 Biological composition <i>Nematostella vectensis</i> embryo . . . . .	2
1.3 Gene regulatory networks . . . . .	3
1.4 Mathematical model . . . . .	3
1.5 Observational data preparation . . . . .	5
1.6 Previous models . . . . .	7
1.6.1 Genikhovich’s model . . . . .	7
1.6.2 Honingh’s model . . . . .	7
1.6.3 Oud’s model . . . . .	8
1.7 Parameter optimization . . . . .	11
1.7.1 Global search: Evolutionary algorithm . . . . .	11
1.7.2 Local search . . . . .	12
1.8 Research question . . . . .	12
<b>2 Methods</b>	<b>13</b>
2.1 Reaction-diffusion equations . . . . .	13
2.2 Mesh initialization . . . . .	15
2.3 Initial gene conditions . . . . .	15

2.4	Parameter optimization . . . . .	16
2.4.1	EA implementation . . . . .	17
2.4.2	Local search implementation: Downhill-Simplex method . . . . .	19
2.5	Simulating knock-down experiments . . . . .	20
<b>3</b>	<b>Experiments and results</b>	<b>21</b>
3.1	Timelapse of the gene expression . . . . .	21
3.2	Final computed gene expressions . . . . .	22
3.3	Fitness evolution . . . . .	22
3.3.1	Evolutionary Algorithm . . . . .	22
3.3.2	Downhill-Simplex method . . . . .	23
3.4	Observational data comparison . . . . .	24
3.5	Optimization results . . . . .	26
<b>4</b>	<b>Discussion</b>	<b>30</b>
4.1	Improper gene expression linearization . . . . .	30
4.2	Simulating both the endoderm and the ectoderm . . . . .	30
4.3	Qualitative comparison knock-down results . . . . .	31
<b>5</b>	<b>Conclusion</b>	<b>33</b>
<b>A</b>	<b>Network results</b>	<b>35</b>
A.1	Network 2.1 . . . . .	36
A.2	Network 2.2 . . . . .	37
A.3	Network 2.3 . . . . .	38
A.4	Network 2.4 . . . . .	39
A.5	Network 2.5 . . . . .	40
A.6	Network 2.6 . . . . .	41
A.7	Network 2.7 . . . . .	42
A.8	Network 3.1 . . . . .	43
A.9	Network 3.2 . . . . .	44
A.10	Network 3.3 . . . . .	45
A.11	Network 3.4 . . . . .	46
A.12	Network 3.5 . . . . .	47
A.13	Network 3.6 . . . . .	48
A.14	Network 3.7 . . . . .	49
A.15	Network 4.1 . . . . .	50
A.16	Network 4.2 . . . . .	51
<b>B</b>	<b>Project documentation</b>	<b>52</b>
	<b>Bibliography</b>	<b>55</b>

# List of Figures

1.1	A fully grown <i>Nematostella vectensis</i> . At maturity, they reach up to 4cm [1]. This species is used to study bilateral embryonic development. . . . .	2
1.2	An embryo of the sea-anemone <i>Nematostella vectensis</i> . Two distinct layers can be seen: The ectoderm layer on the outside and the endoderm layer on the inside. The two layers are separated through the mesoglea. On the left is a slice of the lateral orientation shown. The top, indicated by *, is the oral side of the embryo. The bottom is the aboral side. On the right is an oral-orientated slice shown. The scale bars have a width of 50 $\mu$ m. The images are from He et al. [2]. . . . .	3
1.3	An example of a gene regulatory network with three hypothetical genes: A, B and C. An arrowhead represents activation, while a blunt arrowhead represents inhibition. . . . .	4
1.4	Gene expression in an embryo of <i>Nematostella vectensis</i> . Coloured regions show the gene expression. The oral side is positioned to the left for the lateral orientation. . . . .	6
1.5	An example of the drawn pseudo-cells in an embryo of <i>Nematostella vectensis</i> . The pseudo-cells are collapsed onto the nearest point on the line. The numbers indicate the linearized location. . . . .	6
1.6	The proposed gene regulatory network by Genikhovich [3] of a <i>Nematostella vectensis</i> embryo. This model successfully creates an asymmetric expression, but it requires an artificial Chd restriction during the first 2 hours of simulation time. . . . .	8
1.7	The proposed gene regulatory network by Honingh [4] of a <i>Nematostella vectensis</i> is a continuation of the proposed network by Genikhovich [3]. A hypothetical W gene is introduced. The artificial Chd restriction required by the model of Genikhovich is no longer needed to create an asymmetric expression. However, the model is unable to explain knock-down experiments. . . . .	8
1.8	The computed BMP expressions by the model of Honingh are compared against the BMP expressions observed in the lab. On the left is the wild-type expressions plotted. The simulations match with the observed values. On the right are the knock-down experiments plotted. The simulated data does not match with the observed data. . . . .	9
1.9	The core of the proposed network by Oud [5] of the <i>Nematostella vectensis</i> [5]. This model attempts to simplify the model from Honingh [4] as much as possible. A dashed line indicates that the interaction can either be absent, activation, or inhibition. . . . .	9



2.1	A discretized mesh surface representing the mesoglea of the <i>Nematostella vectensis</i> . Each vertex is a point in space where the reaction-diffusion equations are evaluated. . . . .	15
2.2	Three stages of the W expression initialization. (a) Each vertex is assigned a random uniform number between 0 and 1. (b) The noise is smoothened through the heat equation. (c) A smoothed step function is applied to obtain an asymmetric expression between the oral and aboral side. . . . .	16
2.3	The linearized expression created by Greuell [6] for BMP and Chd in the lateral and oral orientation. . . . .	17
3.1	The BMP expression evolution for Network 3.7 at different time steps. The initial BMP expression is caused by the W initialization. Afterwards, the BMP expression spreads at the oral side until an asymmetric expression is reached at the end. . . . .	22
3.2	The final expression at $t = 50000s$ of BMP, Chd, and W for Network 3.7. BMP and Chd create an asymmetric expression. . . . .	22
3.3	The fitness evolution for the best and average instance per generation of Network 3.7. Drops in fitness are caused by exploratory steps, but a general trend of increased fitness is observed. . . . .	23
3.4	The parameter values of the best agent for each generation of Network 3.7. The first few generations have large parameter changes. Over time the fluctuations in parameter values are reduced. . . . .	24
3.5	The fitness value for each evaluation of the network. The parameters for each evaluation are determined by the Downhill-simplex method. A reduction in fitness is caused by exploratory steps. . . . .	25
3.6	The comparison between the in-situ data and the computational model with the optimized parameters for Network 3.7. The computational results are able to match the in-situ data. . . . .	25
3.7	The comparison between the in-situ data and the computational model with the optimized parameters for Network 3.2. This network is able to create an asymmetric expression, except it is unable to match the exact BMP oral expression with the in-situ data. . . . .	28
3.8	Gene expression comparison between the Chd knock-down in-situ data and the simulation where the Chd production is reduced with a factor of 10. These results are from Network 3.7. The results do not match for any of the expressions or orientations. . . . .	29
4.1	Gene expression in an embryo of <i>Nematostella vectensis</i> after applying Chd knock-down experiments. The oral side is positioned to the left for the lateral orientation. . . . .	32
5.1	The gene regulatory network of Network 3.6. This network was able to replicate the asymmetric expression of the wild-type in-situ data and was most in line with the qualitative comparison against the knock-down data. Therefore, Network 3.6 seems to be the most likely candidate to describe the inner workings of the embryo of <i>Nematostella vectensis</i> . . . . .	34
A.1	Expression levels of Network 2.1 after parameter optimization. . . . .	36
A.2	Expression levels of Network 2.1 after Chd knock-out. . . . .	36
A.3	Expression levels of Network 2.2 after parameter optimization. . . . .	37

A.4	Expression levels of Network 2.2 after Chd knock-out. . . . .	37
A.5	Expression levels of Network 2.3 after parameter optimization. . . . .	38
A.6	Expression levels of Network 2.3 after Chd knock-out. . . . .	38
A.7	Expression levels of Network 2.4 after parameter optimization. . . . .	39
A.8	Expression levels of Network 2.4 after Chd knock-out. . . . .	39
A.9	Expression levels of Network 2.5 after parameter optimization. . . . .	40
A.10	Expression levels of Network 2.5 after Chd knock-out. . . . .	40
A.11	Expression levels of Network 2.6 after parameter optimization. . . . .	41
A.12	Expression levels of Network 2.6 after Chd knock-out. . . . .	41
A.13	Expression levels of Network 2.7 after parameter optimization. . . . .	42
A.14	Expression levels of Network 2.7 after Chd knock-out. . . . .	42
A.15	Expression levels of Network 3.1 after parameter optimization. . . . .	43
A.16	Expression levels of Network 3.1 after Chd knock-out. . . . .	43
A.17	Expression levels of Network 3.2 after parameter optimization. . . . .	44
A.18	Expression levels of Network 3.2 after Chd knock-out. . . . .	44
A.19	Expression levels of Network 3.3 after parameter optimization. . . . .	45
A.20	Expression levels of Network 3.3 after Chd knock-out. . . . .	45
A.21	Expression levels of Network 3.4 after parameter optimization. . . . .	46
A.22	Expression levels of Network 3.4 after Chd knock-out. . . . .	46
A.23	Expression levels of Network 3.5 after parameter optimization. . . . .	47
A.24	Expression levels of Network 3.5 after Chd knock-out. . . . .	47
A.25	Expression levels of Network 3.6 after parameter optimization. . . . .	48
A.26	Expression levels of Network 3.6 after Chd knock-out. . . . .	48
A.27	Expression levels of Network 3.7 after parameter optimization. . . . .	49
A.28	Expression levels of Network 3.7 after Chd knock-out. . . . .	49
A.29	Expression levels of Network 4.1 after parameter optimization. . . . .	50
A.30	Expression levels of Network 4.1 after Chd knock-out. . . . .	50
A.31	Expression levels of Network 4.2 after parameter optimization. . . . .	51
A.32	Expression levels of Network 4.2 after Chd knock-out. . . . .	51

# List of Tables

1.1	The 16 proposed networks by Oud [5] of a <i>Nematostella vectensis</i> . The networks are variations of the core network. . . . .	10
2.1	The different hyperparameters used for the EA. These parameters have previously been used successfully [7]. . . . .	19
3.1	A summary of the results for each network. Three different results are shown. Each result is categorized into three categories: <i>Yes</i> , <i>Maybe</i> , and <i>No</i> . The meaning behind <i>Maybe</i> is different for each result. <i>OG (original)</i> : Does the model show asymmetric expression with the original parameters of Oud [5]? The <i>Maybe</i> results indicate that asymmetric transitions were found, but these did not show in the final expression. <i>OE (optimized expression)</i> : Is the model able to replicate the in-situ data with the optimized expression? <i>Maybe</i> indicates that an asymmetric expression was found, but unable to match with the exact in-situ data. <i>KD (knock-down)</i> : Does the expression match with the knock-down data after the parameters were optimized? <i>Maybe</i> indicates that the result is unclear due to the lack of quantitative analysis. . . . .	27
A.1	Final parameters of Network 2.1 . . . . .	36
A.2	Final parameters of Network 2.2 . . . . .	37
A.3	Final parameters of Network 2.3 . . . . .	38
A.4	Final parameters of Network 2.4 . . . . .	39
A.5	Final parameters of Network 2.5 . . . . .	40
A.6	Final parameters of Network 2.6 . . . . .	41
A.7	Final parameters of Network 2.7 . . . . .	42
A.8	Final parameters of Network 3.1 . . . . .	43
A.9	Final parameters of Network 3.2 . . . . .	44
A.10	Final parameters of Network 3.3 . . . . .	45
A.11	Final parameters of Network 3.4 . . . . .	46
A.12	Final parameters of Network 3.5 . . . . .	47
A.13	Final parameters of Network 3.6 . . . . .	48
A.14	Final parameters of Network 3.7 . . . . .	49
A.15	Final parameters of Network 4.1 . . . . .	50
A.16	Final parameters of Network 4.2 . . . . .	51
B.1	A short description of each file and directory used to run the EA and DS method. . . . .	52

# List of Algorithms

1	Pseudocode of an EA . . . . .	11
---	-------------------------------	----

# Abbreviations

<b>BMP</b>	<b>B</b> one <b>M</b> orphogenetic <b>P</b> rotein
<b>Chd</b>	<b>C</b> hordin
<b>DS</b>	<b>D</b> ownhill <b>S</b> implex
<b>EA</b>	<b>E</b> volutionary <b>A</b> lgorithm
<b>GRN</b>	<b>G</b> ene <b>R</b> egulatory <b>N</b> etwork

# Chapter 1

## Introduction

Embryonic development is a complex process that involves several phases before a fully-grown life form emerges. During this process, limbs, organs, sensory systems and other complex features develop. To better understand the origin of these features, it is important to first understand the initial phases of embryonic development. One of these phases is the emergence of bilateral symmetry.

This thesis will research bilateral embryonic development by looking at the embryo of *Nematostella vectensis*. First, it is described why *Nematostella vectensis* is of interest and what the composition of the embryo is. Thereafter, a mathematical model is outlined to simulate embryonic development and how we can test this model against in-situ data. An overview of previous models is given and what key shortcomings for each of the models were.

This thesis will further explore a set of models, which attempt to explain the gene expression of the *Nematostella vectensis* embryo. The exploration will be performed through a parameter search by an evolutionary algorithm (EA) followed by a local search.

### 1.1 The model organism *Nematostella vectensis*

To study embryonic development, a species is needed which can easily and quickly reproduce. Generally, the fruit-fly *Drosophila melanogaster* is chosen as the animal species for genetic research as it is easily reproduce-able, low maintenance and low-cost [8]. Furthermore, its entire genome has been sequenced [9].

However, studying bilateral embryonic developments from their origin would make more sense. The first species to form a bilaterality should contain only the absolute necessity components and would therefore be more easily understood.

Cnidaria, consisting mostly of anemones and jellyfish, are thought to be the last split between the bilateral and non-bilateral animals [10]. Even though, the Cnidaria do not belong to de bilateral, some species within the Cnidaria possess bilateral symmetry in their gene expression. One of these species is *Nematostella vectensis* [11].

The *Nematostella vectensis* is shown in Figure 1.1. The species is easy to propagate and culture under lab conditions [12]. Additionally, its genome has been sequenced just like *Drosophila melanogaster* [13]. Therefore, the *Nematostella vectensis* is chosen as the model organism to study bilateral embryonic development.

## 1.2 Biological composition *Nematostella vectensis* embryo

During the earliest stages of embryonic development, the embryo is formed from a single sheet of cells: the blastula. This sheet of cells forms a hollow sphere. At this point, the embryo is spherically symmetric.

The first axis is determined through Wnt and  $\beta$ -catenin signalling [14] [15]. This is due to gastrulation of the blastula, where the blastula collapses inwards forming an oral-aboral axis. The gastrula consists of three parts: the endoderm, the ectoderm and the mesoglea. The endoderm is on the inside of the embryo encapsulated by the ectoderm on the outside. The mesoglea is a layer separating the endoderm and ectoderm. Figure 1.2 shows an overview of the embryo. At this point, the embryo is radially symmetric.



FIGURE 1.1: A fully grown *Nematostella vectensis*. At maturity, they reach up to 4cm [1]. This species is used to study bilateral embryonic development.

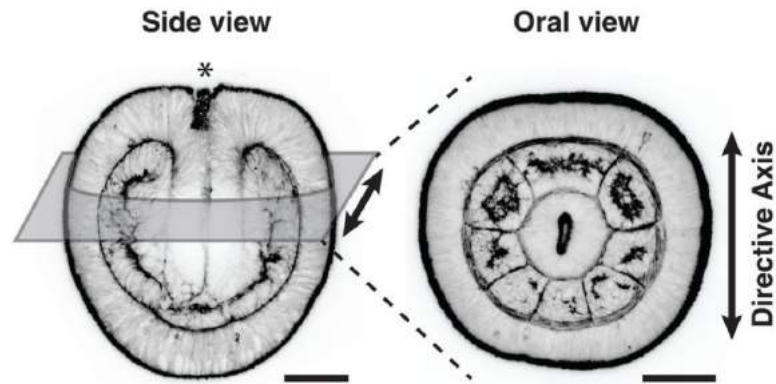


FIGURE 1.2: An embryo of the sea-anemone *Nematostella vectensis*. Two distinct layers can be seen: The ectoderm layer on the outside and the endoderm layer on the inside. The two layers are separated through the mesoglea. On the left is a slice of the lateral orientation shown. The top, indicated by \*, is the oral side of the embryo. The bottom is the aboral side. On the right is an oral-orientated slice shown. The scale bars have a width of  $50\ \mu\text{m}$ . The images are from He et al. [2].

The formation of the secondary axis, perpendicular to the primary axis, is identified through an asymmetric expression of BMPs, consisting of BMP5-8 and DPP, and Chordin [16]. Additionally, other genes such as GDF5l and Gremlin interact with both BMP and Chordin [15].

A mathematical model is set up to further explore the interactions between the various genes. This model should help us with understanding the relationship between the genes and give a better description of embryonic development.

### 1.3 Gene regulatory networks

Gene regulatory networks (GRN) are used to describe the interactions between genes. An example of a GRN can be seen in Figure 1.3. This gene network consists of three genes: A, B and C. A line between two genes describes an interaction between the two genes. An arrow represents the activation of the genes, which increases the gene production rate. In this example, A activates itself and C, and B activates C. On the other hand, a blunt arrow denotes inhibition of the genes, which decreases the production rate and can be seen in the example, where B inhibits A and C inhibits A.

### 1.4 Mathematical model

The gene regulatory networks are modelled through a set of coupled ordinary differential equations. These equations describe the change in gene concentration over time.



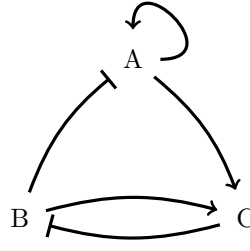


FIGURE 1.3: An example of a gene regulatory network with three hypothetical genes: A, B and C. An arrowhead represents activation, while a blunt arrowhead represents inhibition.

$$\frac{\partial u_{i,j}}{\partial t} = f(u_1, u_2, \dots, u_N) \quad (1.1)$$

where  $u$  is the gene concentration of gene  $i$  at location  $j$ , and  $f(u_1, u_2, \dots, u_N)$  is a source function which depends on one or more genes.

One of these terms in a source function is a diffusion term. The diffusion term is caused by the diffusion of genes, where genes diffuse from a location with a higher concentration to a location with a lower concentration. The diffusion term is described by

$$\text{Diffusion} = D_u \nabla^2 u, \quad (1.2)$$

where  $D_u$  is the diffusion constant of gene  $u$  and  $\nabla^2$  is the Laplace operator. Membrane-bound receptors do not diffuse and therefore have a diffusion constant of zero.

Another term in the source function is the production term. Genes are produced at a production rate  $\rho_u$ , which is different for each gene  $u$ . The production rate is influenced by interactions with other genes. Furthermore, the influence is non-linear. This non-linear influence is captured by the Hill equations [17]

$$\sigma_{A>B} = \frac{A^n}{K_{A>B}^n + A^n} \quad (1.3)$$

$$\bar{\sigma}_{A>B} = \frac{K_{A>B}^n}{K_{A>B}^n + A^n}, \quad (1.4)$$

where  $\sigma$  is the hill equation for the activation and  $\bar{\sigma}$  for inhibition of the gene production,  $n$  the hill constant describing the non-linearity,  $K$  a constant at which the production is half the maximum production, and  $A$  the concentration of gene A. When multiple genes activate or inhibit the production, then the total hill equation is the factor of each individual hill equation

$$\sigma(A, B) = \sigma(A) \cdot \sigma(B) \quad (1.5)$$

Additionally, genes can bind to each other forming ligands. For example, two genes A and B can form a ligand AB, removing genes A and B. This occurs at a binding rate  $k_{\text{on}}^{AB}$  and is proportional to the concentrations of both A and B.

$$\text{binding} = k_{\text{on}}^{AB} \cdot A \cdot B \quad (1.6)$$

Moreover, these ligands are removed through two processes: unbinding and degradation. Unbinding unbinds the ligand into its components, forming the genes A and B again. On the contrary, degradation destroys the ligand into other components other than genes A and B.

$$\text{breakdown} = (k_{\text{off}}^{AB} + \tau) \cdot AB \quad (1.7)$$

where  $k_{\text{off}}^{AB}$  is the unbinding rate and  $\tau$  the degradation rate.

Finally, receptors can degrade over time at a degradation rate *delta*.

## 1.5 Observational data preparation

A computational model has to be tested against experimental data. The experimental data originates from in-situ microscope images of *Nematostella vectensis* as an embryo. These images are created by Genikhovich [3] and processed by Koen [6].

Figure 1.4 shows an example of the in-situ images. The images show an oral and lateral slice of a *Nematostella vectensis* embryo. The oral side is on the left side of the image for the lateral orientation. The coloured regions show gene expression. It can be seen that the coloured regions are much brighter for the Chd gene compared to the BMP gene, indicating that the Chd expression is larger compared to the BMP expression.

The in-situ data are processed by dividing the embryo into a set of pseudo-cells. The average expression is computed for each pseudo-cell. These values are then translated to a line drawn on the cell. This generates an average expression along the embryo. Figure 1.5 shows an example of the pseudo-cells, along with the linearized locations for both the oral and lateral orientation.

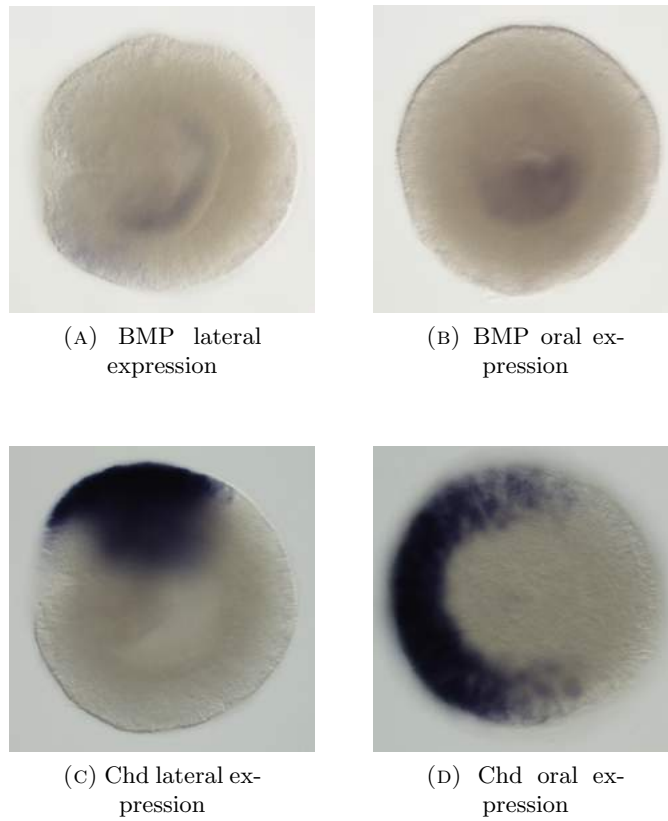


FIGURE 1.4: Gene expression in an embryo of *Nematostella vectensis*. Coloured regions show the gene expression. The oral side is positioned to the left for the lateral orientation.

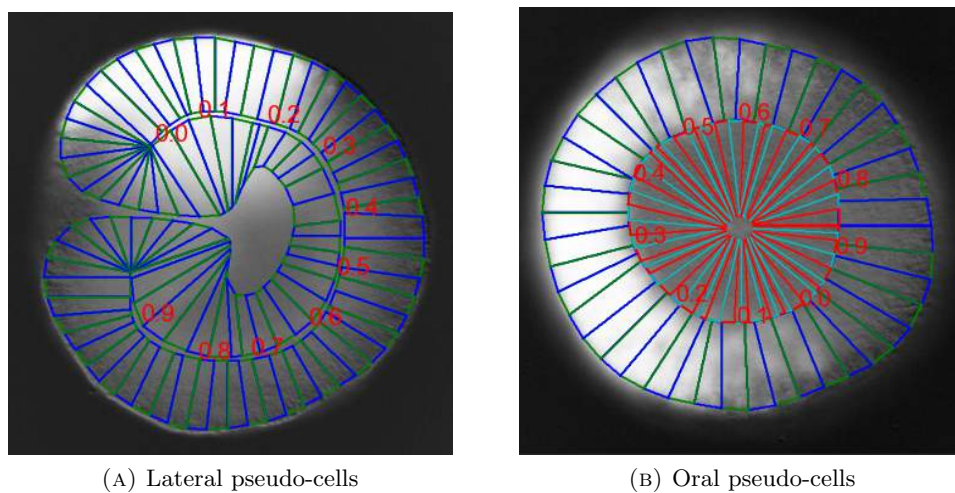


FIGURE 1.5: An example of the drawn pseudo-cells in an embryo of *Nematostella vectensis*. The pseudo-cells are collapsed onto the nearest point on the line. The numbers indicate the linearized location.

Besides wild-type in-situ data, there is also knock-down data available from observations made by Genikhovich [3]. The knock-down data is obtained through morpholino experiments. Morpholinos are designed to block the translation of specific genes, reducing their gene expression.

The wild-type data is used to find parameter values for which the model is accurately able to replicate the gene expressions. The knock-down data is then used to verify the found parameter values of the computational model.

## 1.6 Previous models

Several models have been proposed to replicate the in-situ data from a *Nemostella* embryo. Each model improves on the shortcomings of the ones before. Three different models will be described. The original model by Genikhovich [3], an adaptation by Honingh [4] and a collection of proposed networks by Oud [5].

### 1.6.1 Genikhovich's model

Genikhovich's model [3] is an adaptation of a tested model of the *Drosophila melanogaster* [18]. The *Drosophila melanogaster* and *Nematostella vectensis* networks should have similarities due to their similarities in the BMP-Chordin pathways. The differences in the models are caused by the absence or presence of particular genes. The gene Tsg is not present in *Nemostella* and is therefore removed, on the contrary Gremlin and GDF5 were included. Figure 1.6 shows the gene regulatory network.

This model is able to create an asymmetric expression, however, it does this through an artificial Chordin restriction to one section in the first 2 hours of the simulation time.

### 1.6.2 Honingh's model

The aim of Honingh's model [4] was to remove the artificial Chordin restriction required by Genikhovich's model. This is achieved through the inclusion of a hypothetical W gene. This is supported by the fact that the BMP-Chd signal is dependent on a Wnt signal, from which W is a downstream signal. Figure 1.7 shows the gene regulatory network.

This model has successfully been able to replicate the wild-type data, without the artificial Chordin restriction as shown in Figure 1.8a. It was, however, unable to explain

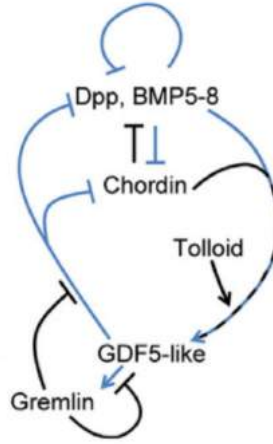


FIGURE 1.6: The proposed gene regulatory network by Genikhovich [3] of a *Nematostella vectensis* embryo. This model successfully creates an asymmetric expression, but it requires an artificial Chd restriction during the first 2 hours of simulation time.

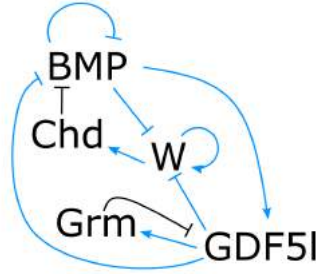


FIGURE 1.7: The proposed gene regulatory network by Honingh [4] of a *Nematostella vectensis* is a continuation of the proposed network by Genikhovich [3]. A hypothetical W gene is introduced. The artificial Chd restriction required by the model of Genikhovich is no longer needed to create an asymmetric expression. However, the model is unable to explain knock-down experiments.

knock-out experiments. The expressions of the simulations did not match with the knock-out data, which can be seen in Figure 1.8b.

### 1.6.3 Oud's model

Further iterations to the model were made by Oud [5], with the aim to simplify the model as much as possible. This would allow extensive parameter research of the model. The model of Honingh was stripped down to the core essence: 3 genes were present with varying activation or inhibition connections. The core model is shown in Figure 1.9. BMP and Chd are always inhibiting each other and BMP inhibits itself. The dashed arrows indicate either activation, inhibition or the absence of a connection.

Sixteen different networks were considered after taking the following assumptions

- W does not inhibit BMP or Chd

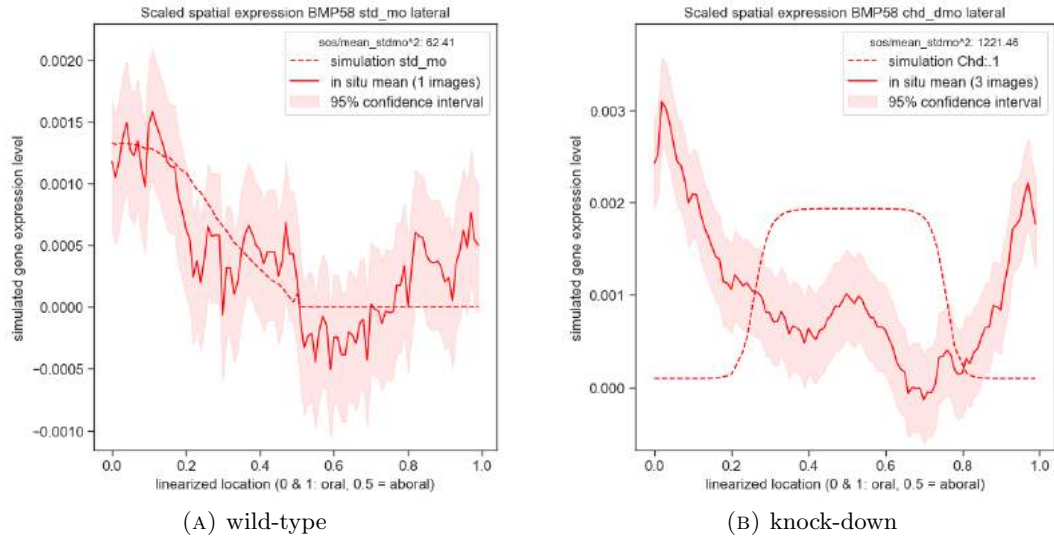


FIGURE 1.8: The computed BMP expressions by the model of Honingh are compared against the BMP expressions observed in the lab. On the left is the wild-type expressions plotted. The simulations match with the observed values. On the right are the knock-down experiments plotted. The simulated data does not match with the observed data.

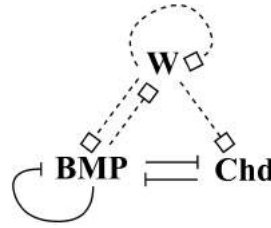


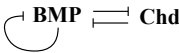
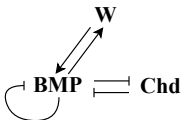
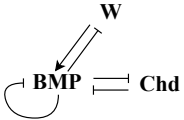
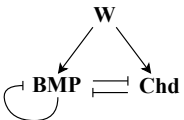
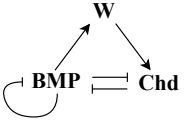
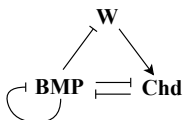
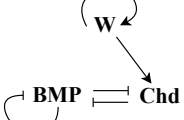
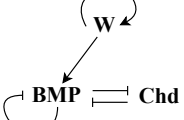
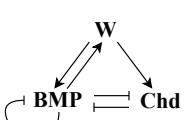
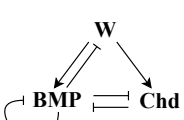
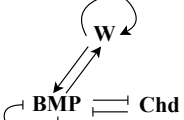
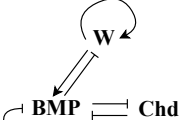
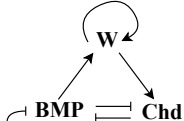
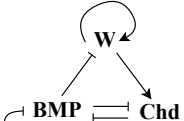
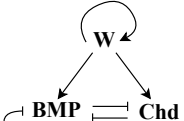
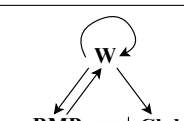
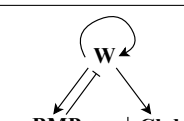
FIGURE 1.9: The core of the proposed network by Oud [5] of the *Nematostella vectensis* [5]. This model attempts to simplify the model from Honingh [4] as much as possible. A dashed line indicates that the interaction can either be absent, activation, or inhibition.

- W does not inhibit itself
- W has to be part of the core network, e.g. W has to activate at least one of BMP or Chd

These networks are displayed in Table 1.1. Several networks were able to show asymmetric expression (Network 3.3, 3.6, 3.7, 4.1, and 4.2), while two networks were able to show asymmetric transitions during the simulation (Network 2.4 and 3.5), but ended in a symmetric solution.

The networks were, however, not tested against the knock-out data. Furthermore, many parameter values were unknown and were empirically set by hand. Therefore, it might be possible that several other networks are able to show asymmetric expression, but were not found during experimentation. Thus, it is essential that the networks are

TABLE 1.1: The 16 proposed networks by Oud [5] of a *Nematostella vectensis*. The networks are variations of the core network.

Core network	 Network 1.1
Two connections	<div>     </div> <div>    </div> <div>         Network 2.1    Network 2.2    Network 2.3    Network 2.4 [I]       </div> <div>         Network 2.5    Network 2.6    Network 2.7       </div>
Three connections	<div>     </div> <div>    </div> <div>         Network 3.1    Network 3.2    Network 3.3 [A]    Network 3.4       </div> <div>         Network 3.5 [I]    Network 3.6 [A]    Network 3.7 [A]       </div>
Four connections	<div>   </div> <div>         Network 4.1 [A]    Network 4.2 [A]       </div>

- [A] marks networks that show an asymmetry
- [I] marks networks that show interesting asymmetric transient dynamics, but do not converge to an asymmetric pattern

systematically tested, such that optimal parameter values are found, which are best able to explain the in-situ data.

## 1.7 Parameter optimization

The parameter exploration is performed in two steps: an evolutionary algorithm and a local search. Both methods attempt to minimize the difference between the simulation results and in-situ data by tweaking the network's parameters.

### 1.7.1 Global search: Evolutionary algorithm

An evolutionary algorithm mimics evolution theory [19]. An initial population is created with different genes. The instances are then tested in their environment. The most successful instances are able to create offspring. The offspring contains a recombination of the parent's genes with mutations applied. This method is able to optimize for the environment due to the selection pressure, while able to escape local maxima through recombination and mutation.

The genes in our case are the parameter values. These parameter values are used in the network and are tested against in-situ data, which is the fitness of the instance. The best-performing instances are able to create new offspring from their parameter values. A schematic overview of this process can be seen in Algorithm 1.

---

**Algorithm 1:** Pseudocode of an EA

---

1. INITIALIZATION: Generate a population with a large range of parameter values
  2. Repeat until some termination criterium is met
    - 2.1. SCORING: Calculate the fitness of each instance
    - 2.2. RANKING: Select the best instances
    - 2.3. RECOMBINATION: Create offspring based on the best instances
    - 2.4. MUTATION: Apply mutations to the offspring
- 

Through careful initialization, the initial population will span a large volume of the solution space, such that the optimal parameter values fall within this span. The mutations and recombinations force the parameters to explore the solution space in search of the global minimum.



### 1.7.2 Local search

A local search explores the solution space locally, where it improves the solution within a local minimum. Therefore, local search is applied to the solutions found by the EA. This strategy has been used successfully before [7]. The EA's responsibility is to, hopefully, find the close to the global minima and the local search then attempts to find the true global minima.

Local search, generally, finds the minima by sampling several points around the initial value. The direction towards the minima is determined from this sampling. This process repeats until the minimum is found or until some termination criterium is met.

## 1.8 Research question

In this report, an EA and local search will be implemented to study the parameters of each of the sixteen networks of Steven. The aim is to match the gene expressions of the already established asymmetric networks with the available in-situ data. Furthermore, the non-asymmetric networks will be tested in an attempt to find whether these networks are able to show asymmetric expression under the right parameters and match with the in-situ data. Finally, knock-down experiments will be performed and compared to knock-down in-situ data. These knock-down experiments are used to verify the possible existence of the networks.

## Chapter 2

# Methods

Two distinct research fields are needed to study the possible asymmetric properties of each of the 16 proposed networks by Oud [5].

First, a computational model is set up. This computational model consists of the reaction-diffusion equations tied to each GRN, a spatial discretization of the computational domain, and the initialization of the gene concentrations. This is performed on COMSOL V6.1 [20].

Secondly, each GRN is evaluated and optimized against the in-situ data through parameter optimization. The parameter optimization is applied first by an EA followed by a local search.

### 2.1 Reaction-diffusion equations

An example of the reaction-diffusion equations is captured in equations 2.1 to 2.5. These equations show the general form for all networks, shown in Table 1.1, except the core network. The core network contains all terms, except terms dependent on  $W$ .

$$\begin{aligned}
\frac{\partial c_{\text{BMP}}}{\partial t} = & \underbrace{D\nabla^2 c_{\text{BMP}}}_{\text{BMP diffusion term}} + \underbrace{\rho_{\text{BMP}}\sigma_{\text{BMP}}}_{\text{BMP production}} - \underbrace{k_{\text{on}}^{\text{BMP-Chd}} c_{\text{BMP}} c_{\text{Chd}}}_{\text{BMP-Chd binding}} \\
& + \underbrace{(k_{\text{off}}^{\text{BMP-Chd}} + \tau) c_{\text{BMP-Chd}}}_{\text{BMP-Chd dissociation and breakdown}} - \underbrace{k_{\text{on}}^{\text{BMP-R}} (R_{\text{tot}}^{\text{BMP}} - c_{\text{BMP-R}}) c_{\text{BMP}}}_{\text{Binding BMP to BMP-R}} \\
& + \underbrace{k_{\text{off}}^{\text{BMP-R}} c_{\text{BMP-R}}}_{\text{Dissociation BMP from BMP-R}}
\end{aligned} \tag{2.1}$$

$$\frac{\partial c_{\text{BMP-R}}}{\partial t} = \underbrace{k_{\text{on}}^{\text{BMP-R}} (R_{\text{tot}}^{\text{BMP}} - c_{\text{BMP-R}}) c_{\text{BMP}}}_{\text{Binding BMP to BMP-R}} - \underbrace{(k_{\text{off}}^{\text{BMP-R}} + \delta_{\text{BMP-R}}) c_{\text{BMP-R}}}_{\text{BMP-R dissociation and degradation}} \tag{2.2}$$

$$\begin{aligned}
\frac{\partial c_{\text{Chd}}}{\partial t} = & \underbrace{D\nabla^2 c_{\text{Chd}}}_{\text{Chd diffusion term}} + \underbrace{\rho_{\text{Chd}}\sigma_{\text{Chd}}}_{\text{Chd production}} - \underbrace{k_{\text{on}}^{\text{BMP-Chd}} c_{\text{BMP}} c_{\text{Chd}}}_{\text{BMP-Chd binding}} \\
& + \underbrace{k_{\text{off}}^{\text{BMP-Chd}} c_{\text{BMP-Chd}}}_{\text{Dissociation BMP-Chd}}
\end{aligned} \tag{2.3}$$

$$\begin{aligned}
\frac{\partial c_{\text{BMP-Chd}}}{\partial t} = & \underbrace{D\nabla^2 c_{\text{BMP-Chd}}}_{\text{BMP-Chd diffusion term}} + \underbrace{k_{\text{on}}^{\text{BMP-Chd}} c_{\text{BMP}} c_{\text{Chd}}}_{\text{BMP-Chd binding}} \\
& - \underbrace{(k_{\text{off}}^{\text{BMP-Chd}} + \tau) c_{\text{BMP-Chd}}}_{\text{BMP-Chd dissociation and breakdown}}
\end{aligned} \tag{2.4}$$

$$\frac{\partial c_{\text{W}}}{\partial t} = \underbrace{\rho_{\text{W}}\sigma_{\text{W}}}_{\text{W production}} - \underbrace{\delta_{\text{W}} c_{\text{W}}}_{\text{W degradation}} \tag{2.5}$$

The differences in the networks are captured in the production terms,  $\sigma_{\text{BMP}}$ ,  $\sigma_{\text{Chd}}$ , and  $\sigma_{\text{W}}$ . The production is different due to the different activation and inhibition relations. For example, Network 3.7 implements Equations 2.6 to 2.8 for the production terms.

$$\sigma_{\text{BMP}} = \bar{\sigma}_{\text{BMP-R} > \text{BMP}} \sigma_{\text{W} > \text{BMP}} \tag{2.6}$$

$$\sigma_{\text{Chd}} = \bar{\sigma}_{\text{BMP-R} > \text{Chd}} \sigma_{\text{W} > \text{Chd}} \tag{2.7}$$

$$\sigma_{\text{W}} = \sigma_{\text{W} > \text{W}} \tag{2.8}$$

The backwards differentiation formula [21] is used to solve the reaction-diffusion equations. Automatic time stepping is used to increase performance. The simulation runs for  $5 \cdot 10^4$  seconds.

## 2.2 Mesh initialization

The gene regulatory networks are implemented on a discretized mesh surface, see Figure 2.1. This mesh surface represents the mesoglea, a layer between the endoderm and ectoderm. The surface follows the curvature of a sphere, where on one end a slice is cut off. This is the oral side of the embryo. The sphere has a diameter of  $160\ \mu\text{m}$ , with the slice being removed at  $65\ \mu\text{m}$  from its centre. The surface is built from 758 triangles, using the `Normal` element size of COMSOL.

## 2.3 Initial gene conditions

The reaction-diffusion equations require an initial gene expression. All compartments used an initial concentration of 0 across the computational domain since they did not alter the results of the final simulation [4]. Only W required an initial concentration profile. This was achieved in three steps.

First, all vertices are assigned a random uniform number between 0 and 1, as shown in Figure 2.2a. The same seed is used for every mesh initialization to make the results consistent. Secondly, the expression is smoothened by applying the heat equation for 50 seconds

$$\frac{\partial c}{\partial t} = \frac{\partial^2 c}{\partial x^2} + \frac{\partial^2 c}{\partial y^2} + \frac{\partial^2 c}{\partial z^2}, \quad (2.9)$$

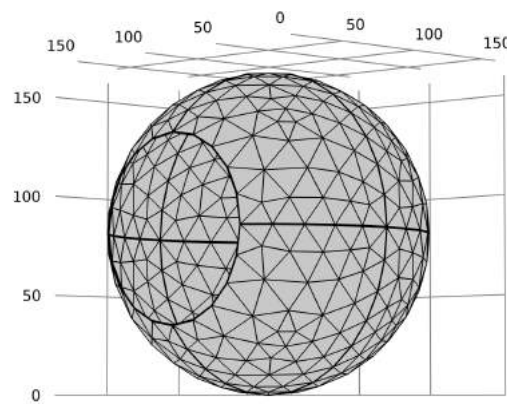


FIGURE 2.1: A discretized mesh surface representing the mesoglea of the *Nematostella vectensis*. Each vertex is a point in space where the reaction-diffusion equations are evaluated.

where  $c$  is the W concentration. Figure 2.2b shows the smoothened noise. After the smoothening period, a transformation of the W expression is applied, which subtracts the minimum W expression over the entire domain of all the values.

$$c_{\text{new}} = c_{\text{old}} - \min(c_{\text{old}}) \quad (2.10)$$

Finally, a smoothened step function from 1 to 0 is applied around the z-axis to localize the W expression to the oral side of the embryo, as seen in Figure 2.2c. The smoothing zone is  $10 \mu\text{m}$  in radius. Therefore, a smooth transition is achieved from the oral to the aboral side.

## 2.4 Parameter optimization

The parameters of the networks are optimized such that the error over the gene expression is minimized. The target linearized expression data can be seen in Figure 2.3.

The in-situ data contains a lateral and an oral slice of the embryo. Therefore, the 3D computational model is also sliced into a lateral and oral slice. From these slices, the relative squared error is computed

$$\epsilon_{(g,o)} = \sum_{i=0}^N \frac{(y_i - p_i)^2}{(y_i - \bar{y})^2}, \quad (2.11)$$

where  $\epsilon_{(g,o)}$  is the relative squared error of gene  $g$  and orientation  $o$ ,  $y$  is a list of the in-situ expression,  $\bar{y}$  the average in-situ expression, and  $p$  is the predicted computational expression. The values for  $y$  and  $p$  are unique to each gene  $g$  and orientation  $o$ . The

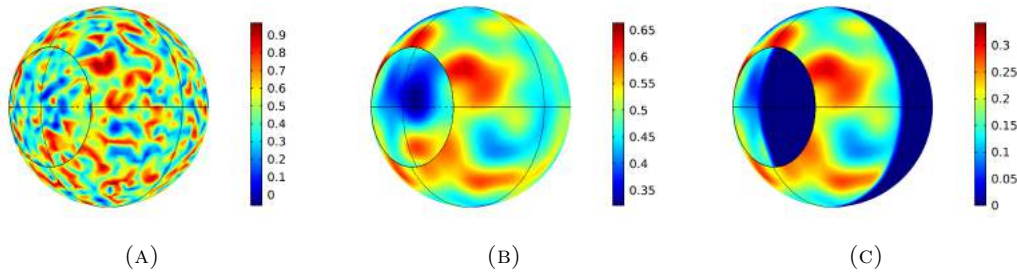


FIGURE 2.2: Three stages of the W expression initialization. (a) Each vertex is assigned a random uniform number between 0 and 1. (b) The noise is smoothened through the heat equation. (c) A smoothed step function is applied to obtain an asymmetric expression between the oral and aboral side.

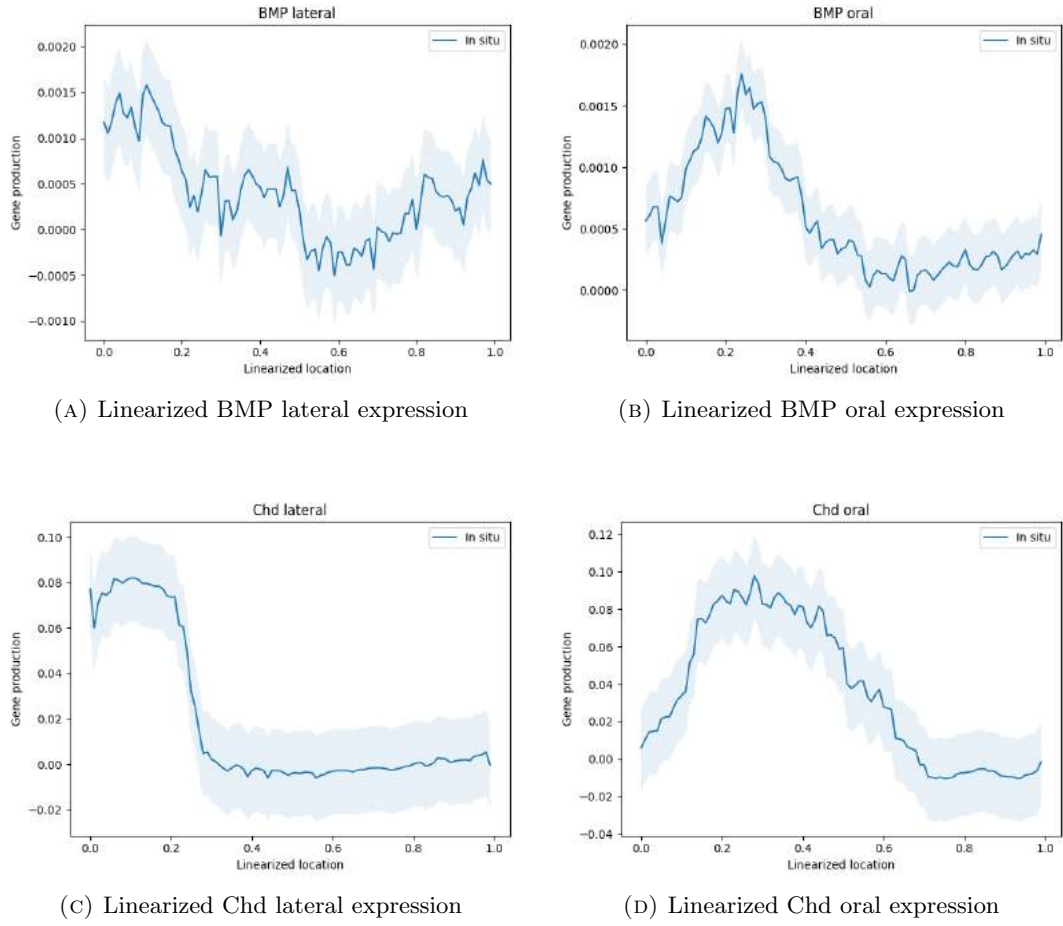


FIGURE 2.3: The linearized expression created by Greuell [6] for BMP and Chd in the lateral and oral orientation.

relative squared error was chosen since it provides a better comparison for multiple different genes since the BMP and Chd expression levels differ in an order of magnitude.

The total error of an instance is the sum of the BMP and Chd expression for both the oral and lateral orientations. A smaller fitness equates to a larger fitness. Therefore, the fitness of an instance is the inverse of the total error.

$$\text{fitness} = \left( \sum_{g \in \{\text{BMP}, \text{Chd}\}} \sum_{o \in \{\text{Lateral}, \text{Oral}\}} \epsilon_{(g,o)} \right)^{-1} \quad (2.12)$$

#### 2.4.1 EA implementation

A self-adaptive EA was chosen to find an optimal set of parameters for each network [22]. This strategy has proved to be successful in previous research [7]. The EA uses self-adaptive mutation steps, which are controlled by the best-performing instances.

Initially, an initial population of size  $\lambda$  is created. One instance holds the exact same values as used in the work of Steven. This was done since it guarantees that at least one instance will hold an asymmetric expression. The other  $n - 1$  instances are assigned a parameter vector according to

$$\mathbf{x} = \mathbf{x}_{\text{init}} \cdot 10^{U(-1,1)}, \quad (2.13)$$

where  $\mathbf{x}$  is the parameter vector,  $\mathbf{x}_{\text{init}}$  the original parameter vector from the work of Oud [5],  $U(-1,1)$  a vector whose values are generated from a random uniform distribution in the range of -1 and 1. This range is empirically determined. Larger ranges created a very large solution space wherein it became too difficult to find asymmetric regions. Smaller ranges resulted in too little exploration.

The step-size control parameter controls the mutations steps per parameter and is unique for each instance. If an instance is performing great due to large mutations, then its offspring will also have large mutations. However, if the instance is performing well due to small mutations, then its offspring will have small mutations. This allows the EA to adapt its mutations to the environment. The initial value of the step-size control parameter is computed based on the initial parameter values

$$\sigma'_k = \frac{(\bar{\mathbf{x}}_k - \mathbf{x}_k)}{\sqrt{n}}, \quad (2.14)$$

where  $n$  is the number of parameters in the model.

The population is tested for its fitness for each generation. The instances are sorted according to their fitness. Then, the offspring is created where  $\mu$  instances are created through recombination. The parameter values of these  $\mu$  instances are assigned according to

$$\mathbf{x}'_k = \mathbf{x}_i + \gamma(\mathbf{x}_1 - \mathbf{x}_{i+1}), \quad (2.15)$$

where  $\mathbf{x}'_k$  is the parameter vector of the new offspring,  $\mathbf{x}_i$  is the parameter vector of the  $i$ -th best-performing instance and  $\gamma$  a hyper-parameter.

The remaining  $\lambda - \mu$  instances are created through mutations applied to the best  $\mu$  agents.

At first, the step-size control parameter is updated

$$\sigma'_{k,j} = \sigma_{i,j} e^{\tau' N(0,1) + \tau N_j(0,1)}, \quad (2.16)$$

where  $\tau' = \phi / \sqrt{2\sqrt{n}}$  and  $\tau = \phi / \sqrt{2n}$  are the learning rates per instance and per parameter, respectively, with  $\phi$  a hyper-parameter.  $N(0, 1)$  is a random variable generated from a Gaussian distribution with zero mean and a standard deviation of 1. The value of  $N(0, 1)$  is shared between all parameters of this instance, while  $N_j(0, 1)$  is unique for this parameter.

Secondly, the mutations are applied with the updated step-size control parameters

$$\mathbf{x}'_k = \mathbf{x}_i + \boldsymbol{\sigma}'_k N(0, 1) \quad (2.17)$$

At last, the step-size control parameter is reduced through a smoothing factor  $\alpha$

$$\boldsymbol{\sigma}'_k = \boldsymbol{\sigma}_i + \alpha(\boldsymbol{\sigma}'_k - \boldsymbol{\sigma}_i) \quad (2.18)$$

An overview of the EA hyper-parameters can be seen in Table 2.1 and are taken from Fomekong-Nanfack et al. [7].

The EA used a population size of 50 and runs for 50 generations. These values were found empirically. 50 generations were deemed enough as the fitnesses of the population were able to converge within the 50 generations as shown in Figure 3.3. A larger population size with more generations could have been used, but this would have increased the computational cost. It was judged that the additional computational cost outweighed the possibility of any small increments of fitness.

#### 2.4.2 Local search implementation: Downhill-Simplex method

The solution found by the EA is further improved upon through a local search. The local search method used was the Downhill-Simplex (DS) method [23]. The DS method is implemented through the python module `scipy.optimize.fmin` [24].

TABLE 2.1: The different hyperparameters used for the EA. These parameters have previously been used successfully [7].

Symbol	Value	Description
$\alpha$	0.2	Smoothing factor
$\phi$	1	Expected rate of convergence
$\mu$	0.2	Fraction of individuals undergoing recombination



The DS method requires an initial simplex. This simplex is a set of starting parameter vectors. The set should be of size  $n + 1$ , where  $n$  is the number of parameters of the network. The parameter vectors are obtained by the EA. The best  $n + 1$  performing instances build the simplex.

The simplex encloses a region, then this region is iteratively reduced to a minimum value. The target is to find a maximum value of the fitness (Equation 2.12). Therefore, the DS method attempts to minimize the negative of the fitness.

## 2.5 Simulating knock-down experiments

The knock-out experiments, described in Section 1.5, are simulated on the best solution found after the EA and the DS method. The knock-out experiments are implemented in the model by tweaking the production rate of the affected gene. This is achieved by reducing the production rate of the knock-out gene.

$$\rho_{\text{gene,new}} = \frac{\rho_{\text{gene,old}}}{f}, \quad (2.19)$$

where  $f$  is the reduction factor. Different reduction factors have been tested.

## Chapter 3

# Experiments and results

All sixteen proposed networks from Section 1.6.3 are optimized against the observational in-situ data. The in-situ data process is described in Section 1.5. One network (Network 3.7) will be used as a case study, all intermediate results will be shown for this network. These intermediate results include

- The BMP expression over time
- The final expression for BMP, Chd, and W
- The fitness evolution for both the EA as well as the local search
- The parameter evolution of each parameter for the best agent of each generation.
- The comparison between the computed expression and the in-situ data.

At the end of the section, there is a summary of the final results for all networks, which include the final parameters, the final BMP, Chd and W expressions and the final BMP, Chd and W expressions after Chd knock-out experiments.

### 3.1 Timelapse of the gene expression

Figure 3.1 shows the BMP expression evolution of network 3.7. Initially, localized spots of BMP expression emerge due to the initialized W expression. These localized spots quickly grow and merge into each other forming a large asymmetry between the oral and aboral sides. This contrast is formed due to the asymmetric W expression. Finally, the secondary asymmetric axis is formed due to small variances in the BMP expression.

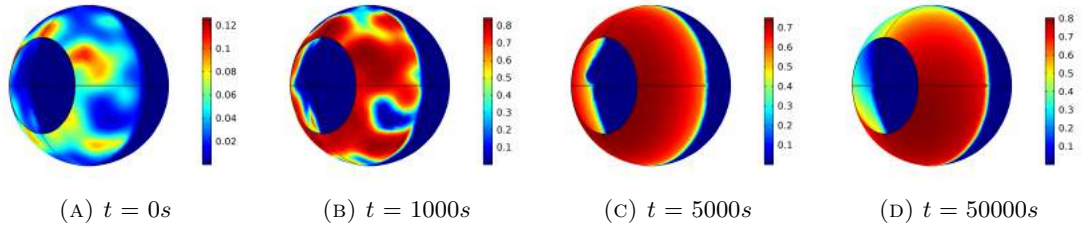


FIGURE 3.1: The BMP expression evolution for Network 3.7 at different time steps. The initial BMP expression is caused by the W initialization. Afterwards, the BMP expression spreads at the oral side until an asymmetric expression is reached at the end.

## 3.2 Final computed gene expressions

The expressions for BMP, Chd and W are captured after simulating the network for 50000 seconds. The results are shown in Figure 3.2. Oral and lateral slices are then taken from the BMP and Chd domains. These slices are compared against the linearized in-situ data from Figure 2.3. The fitness score is then calculated by Equation 2.12.

## 3.3 Fitness evolution

The models are optimized through 2 steps: an EA followed by a local search, as described in sections 2.4.1 and 2.4.2, respectively. The EA attempts to find the region at which the global optimum resides. Then the local search iterates further on the EA solution.

### 3.3.1 Evolutionary Algorithm

Initially, the models are optimized through the EA described in Section 2.4.1. An initial population with 50 different instances is created. The instances are evolved over 50 generations. The fitness evolution can be seen in Figure 3.3.

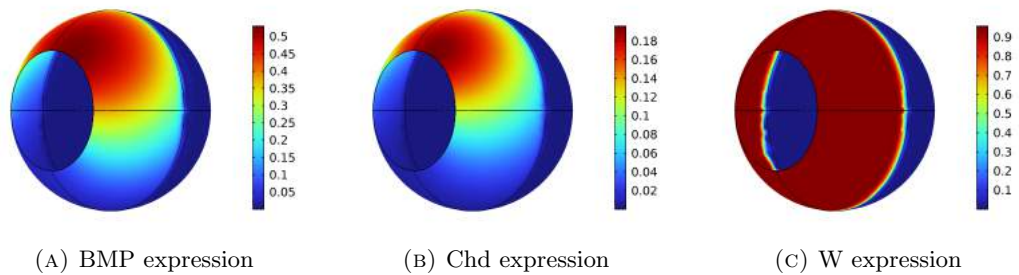


FIGURE 3.2: The final expression at  $t = 50000s$  of BMP, Chd, and W for Network 3.7. BMP and Chd create an asymmetric expression.

An increase in fitness is observed as the number of generations increases, caused by successful recombinations and mutations. Temporary decreases in fitness are because of failed mutations.

It can be seen that the best fitness of each generation converges when the number of generations increases. This indicates that the system is unable to find further improvements, even though the population still undergoes fairly large mutations. This can be seen due to the fluctuations in the average fitness.

Figure 3.4 shows how the parameters change for the best instance for each generation. Initially, the parameters change the most. The changes reduce over time due to two reasons. The first reason is the smoothing factor, which reduces the mutation steps. Secondly, the best parameters have less room to explore as they approach the optimal solution. Some parameters still have relatively large mutations in the final generations, indicating that the model is not sensitive to these parameters.

### 3.3.2 Downhill-Simplex method

The best parameters found by the EA are further improved by the Downhill-Simplex local search. An initial simplex is formed from the best  $n + 1$  instances of the EA search, where  $n$  is the number of parameters for the model. The results of the Downhill-Simplex are found in Figure 3.5.

The fitness is captured for each iteration of the Downhill-Simplex method. The drop-offs in fitness are caused by the exploration steps of the method. The DS is only able to

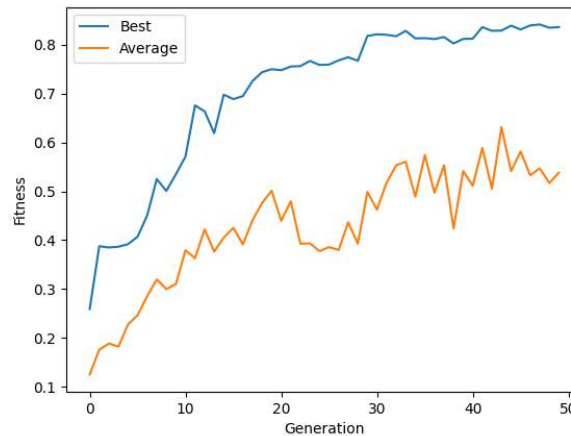


FIGURE 3.3: The fitness evolution for the best and average instance per generation of Network 3.7. Drops in fitness are caused by exploratory steps, but a general trend of increased fitness is observed.

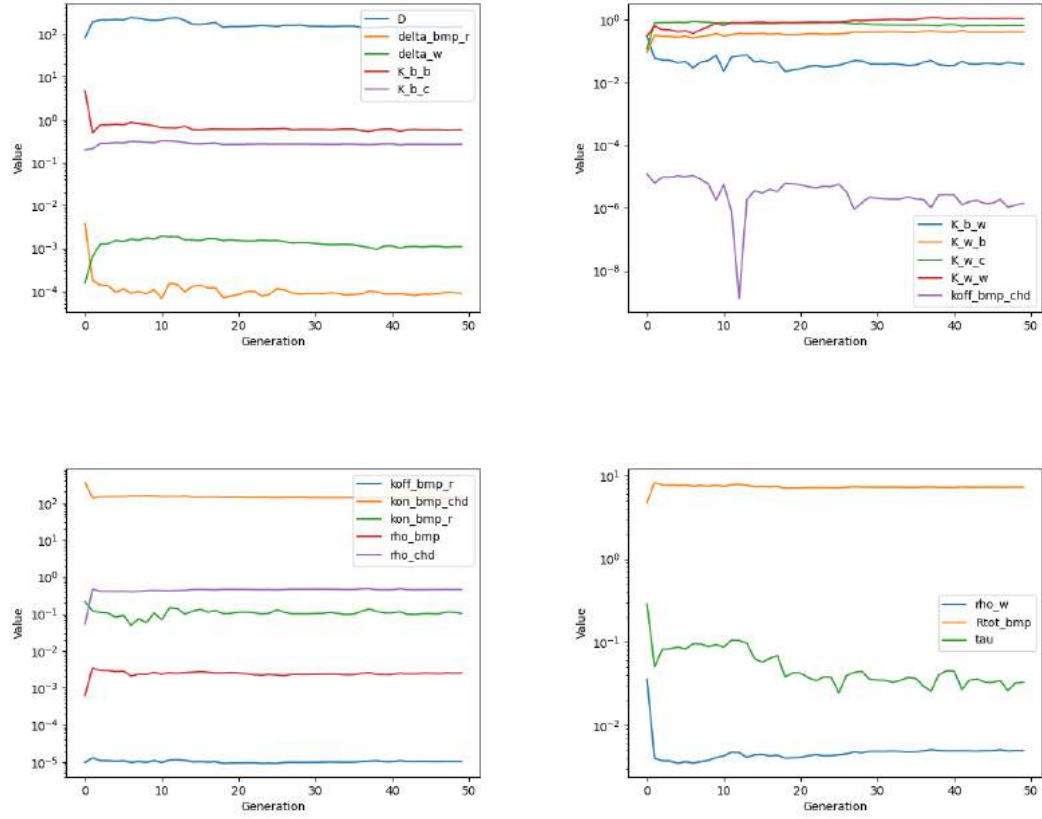


FIGURE 3.4: The parameter values of the best agent for each generation of Network 3.7. The first few generations have large parameter changes. Over time the fluctuations in parameter values are reduced.

find a very small fitness improvement. Therefore the DS method was not executed for all networks as it is only able to find significant fitness gains for the networks which did run DS.

### 3.4 Observational data comparison

The final comparison between the in-situ data and network after parameter optimization is shown in Figure 3.6. The network is able to replicate the gene expressions for both BMP and Chd in both the lateral and oral orientations. Therefore, Network 3.7 is a possible candidate to explain the gene interactions of the *Nematostella vectensis* embryo.

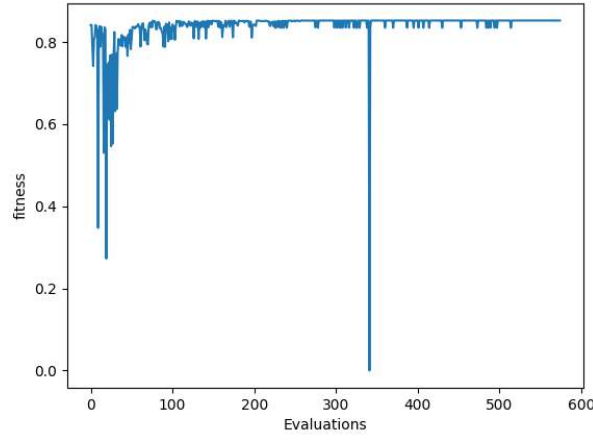
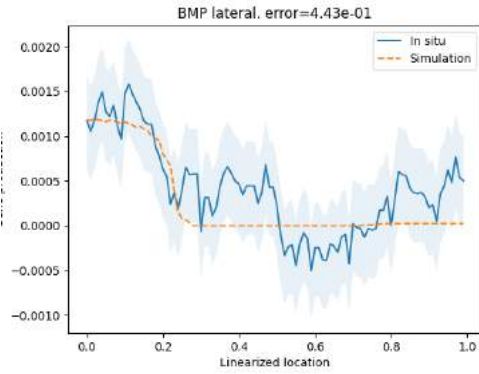
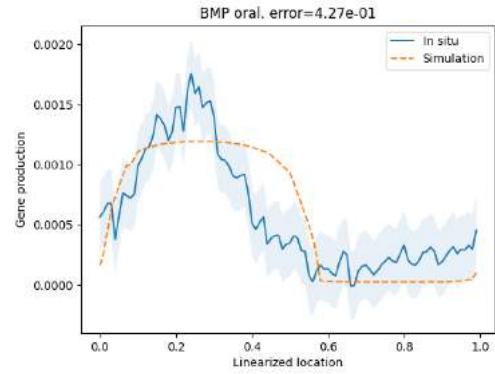


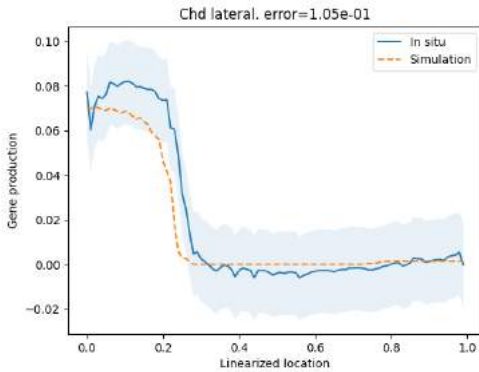
FIGURE 3.5: The fitness value for each evaluation of the network. The parameters for each evaluation are determined by the Downhill-simplex method. A reduction in fitness is caused by exploratory steps.



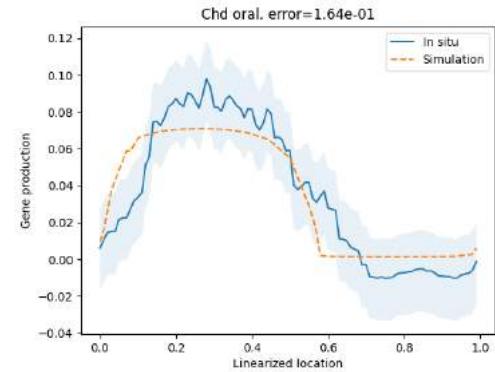
(A) Linearized BMP lateral expression



(B) Linearized BMP oral expression



(C) Linearized Chd lateral expression



(D) Linearized Chd oral expression

FIGURE 3.6: The comparison between the in-situ data and the computational model with the optimized parameters for Network 3.7. The computational results are able to match the in-situ data.

### 3.5 Optimization results

The final results for all networks after optimization by the EA are displayed in Appendix A. These results include the final parameters, the final BMP, Chd and W expressions and the final BMP, Chd and W expressions after Chd knock-down experiments.

A summary of the results of each network is displayed in Table 3.1. These results show whether the network was able to create an asymmetric expression before and after optimization by the EA.

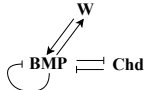
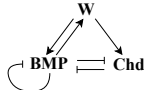

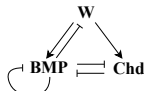
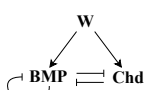
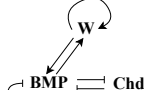
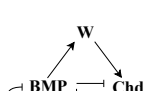

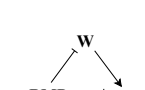



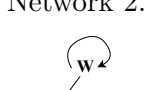
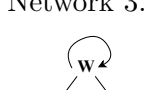

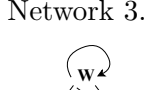
Originally, five networks (Network 3.3, 3.6, 3.7, 4.1, and 4.2) were able to show asymmetric expression with the original values of Oud [5], while two networks (Network 2.4 and 3.5) showed asymmetric dynamics. Through parameter optimization, the asymmetric networks were able to match the computed expression with the in-situ data. Furthermore, the two networks with asymmetric dynamics were also able to create a stable asymmetric pattern conforming to the in-situ data. Additionally, one new network (Network 2.5) was found, which was able to replicate the asymmetric in-situ expression. Therefore, in total 8 different networks were able to replicate the in-situ data.

Four other networks (Network 2.3, 2.6, 3.1, 3.2) were also able to show asymmetric expressions. These networks were, however, unable to reproduce the same patterns as the in-situ data. An example of the pattern mismatch is shown in Figure 3.7 for Network 3.2.

Initially, all asymmetric networks needed W to be self-activating, but this is no longer required as additional networks were found without the self-activation.

An attempt was made to reduce the number of candidates. This attempt compared the knock-out simulations with the knock-out in-situ data. None of the networks were, however, able to match the simulations against the in-situ data. An example of the mismatch between the computed knock-down results and the in-situ data of Network 3.7 is shown in Figure 3.8. Both BMP and Chordin do not match with the knock-down data for the oral and lateral orientations. Possible explanations for this mismatch will be explained in the Discussion.

TABLE 3.1: A summary of the results for each network. Three different results are shown. Each result is categorized into three categories: *Yes*, *Maybe*, and *No*. The meaning behind *Maybe* is different for each result. *OG (original)*: Does the model show asymmetric expression with the original parameters of Oud [5]? The *Maybe* results indicate that asymmetric transitions were found, but these did not show in the final expression. *OE (optimized expression)*: Is the model able to replicate the in-situ data with the optimized expression? *Maybe* indicates that an asymmetric expression was found, but unable to match with the exact in-situ data. *KD (knock-down)*: Does the expression match with the knock-down data after the parameters were optimized? *Maybe* indicates that the result is unclear due to the lack of quantitative analysis.

Network	OG	OE	KD	Network	OG	OE	KD
 Network 2.1	N	N	N	 Network 3.1	N	M	M
 Network 2.2	N	N	N	 Network 3.2	N	M	M
 Network 2.3	N	M	N	 Network 3.3	Y	Y	N
 Network 2.4	M	Y	M	 Network 3.4	N	N	N
 Network 2.5	N	Y	M	 Network 3.5	M	Y	M
 Network 2.6	N	M	N	 Network 3.6	Y	Y	M <sup>1</sup>
 Network 2.7	N	N	N	 Network 3.7	Y	Y	M
 Network 4.1	Y	Y	M	 Network 4.2	Y	Y	N

1. Network 3.6 appears to be able to match with the knock-down data due to a low gradient in BMP expression.



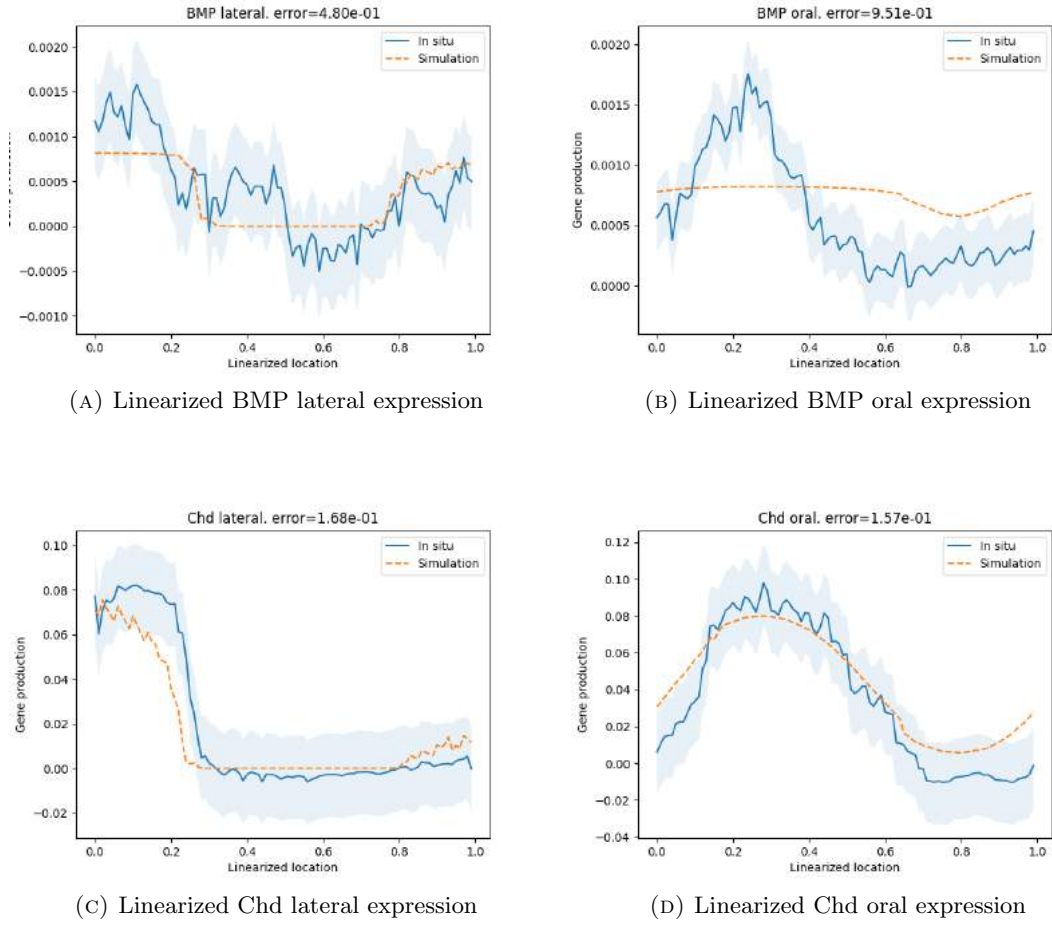
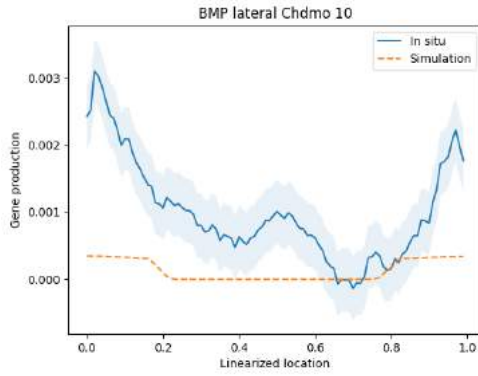
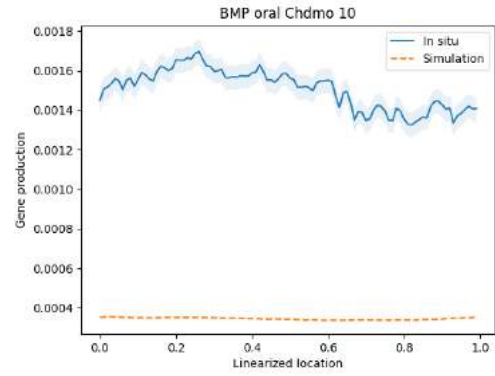


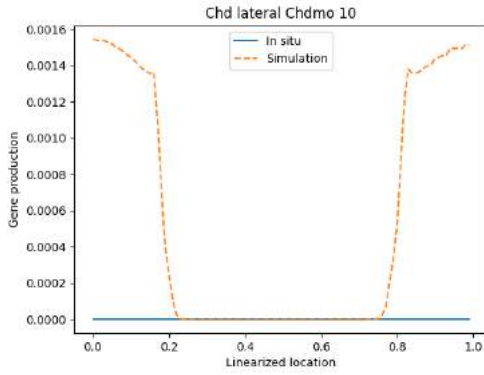
FIGURE 3.7: The comparison between the in-situ data and the computational model with the optimized parameters for Network 3.2. This network is able to create an asymmetric expression, except it is unable to match the exact BMP oral expression with the in-situ data.



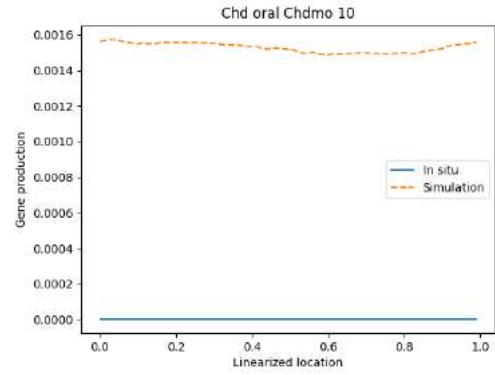
(A) Linearized BMP lateral expression



(B) Linearized BMP oral expression



(C) Linearized Chd lateral expression



(D) Linearized Chd oral expression

FIGURE 3.8: Gene expression comparison between the Chd knock-down in-situ data and the simulation where the Chd production is reduced with a factor of 10. These results are from Network 3.7. The results do not match for any of the expressions or orientations.

## Chapter 4

# Discussion

Eight of the sixteen proposed networks by Oud [5], as described in Section 1.6.3, were able to replicate the wild-type in-situ data. None were, however, able to replicate the knock-down experiments. Two possible solutions to this problem will be described: improper gene expression linearization and an extension to the computational mesh. Furthermore, a qualitative comparison between the knock-out data and computational results will be made.

### 4.1 Improper gene expression linearization

The data extraction linearized the expression domains of the in-situ images onto a singular line drawn on the embryo, as described in Section 1.5. This process collapses the pseudo-cells of both the endoderm and the ectoderm layer onto one. Therefore, the distinction between the layers is lost. This causes problems since the two layers have distinct gene expression profiles, as can be seen in Figure 1.4

To rectify this problem, a solution is proposed where the pseudo-cells are instead collapsed onto two lines; one for the endoderm and one for the ectoderm. This keeps the two layers separate.

### 4.2 Simulating both the endoderm and the ectoderm

The current model would need to be adjusted to work with the proposed adaptation of the data extraction. The current model only outputs a singular layer, the mesoglea,

while the proposed adaptation requires two layers. A natural extension to the computational mesh would therefore include two meshes: one for the ectoderm and one for the endoderm. The networks would be simulated on both layers.

The two layers would interact with each other through the diffusion of the genes, which represents the mesoglea layer. This diffusion parameter would have to be much less than the diffusion parameter of the endoderm and ectoderm layer, otherwise, the layers would diffuse too much and become identical.

### 4.3 Qualitative comparison knock-down results

A quantitative comparison between the knock-out data and computational results showed that none of the sixteen networks were able to replicate the results of the knock-down experiments. However, this mismatch might be caused due to the merger of the endoderm and ectoderm layers during the data preparation. Therefore, an attempt at a qualitative comparison is made.

Figure 4.1 shows the in-situ Chd knock-down experiments. It can be seen that the Chd expression is localized on the oral side of the embryo. This Chd expression is radically symmetric, which can be seen from the oral expression. The BMP expression is much less explicit. Although, the expression does not appear to be localized to either side of the embryo. Instead, it seems to appear throughout the entire embryo.

These observations are compared against the knock-out simulations of the eight networks which matched with the wild-type in-situ data (Network 2.4, 2.5, 3.3, 3.5, 3.6, 3.7, 4.1, and 4.2). An overview of the results can be seen in Table 3.1. Networks 2.4, 2.5, 3.6, 3.7, and 4.1 show an asymmetric Chd expression on the oral side, which matches with the observed Chd expression. Only Network 3.6 shows a BMP expression with a low gradient between the oral- and aboral side. The other networks show a larger gradient between the two sides.

From these observations, it appears that Network 3.6 is the most likely candidate for describing the gene network of a *Nematostella vectensis* embryo. A quantitative analysis would, however, need to be applied to make sure that gene expression values match with the knock-down in-situ data.

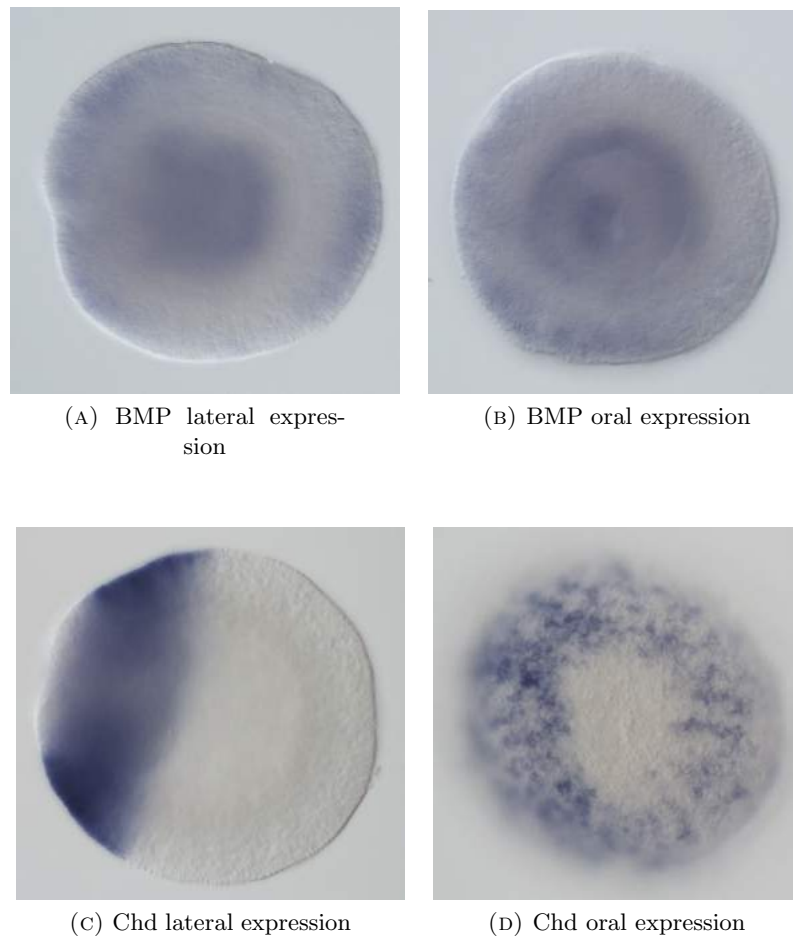


FIGURE 4.1: Gene expression in an embryo of *Nematostella vectensis* after applying Chd knock-down experiments. The oral side is positioned to the left for the lateral orientation.

## Chapter 5

# Conclusion

The sixteen networks proposed by Oud [5] were optimized through an EA in an attempt to match the gene expressions of the networks with the asymmetric in-situ data. Originally, five networks showed asymmetric expressions but did not match with the exact expression profile of the in-situ data. Furthermore, two other networks showed asymmetric transitions. After the EA, these seven networks were able to replicate the in-situ data. Additionally, one new network was also able to show the asymmetric in-situ data, which previously had not been found. Therefore, eight networks complied with the in-situ data. Moreover, the EA was able to find four other networks which showed asymmetric expressions. These four networks were, however, unable to replicate the exact expression profiles of the in-situ data.

A further selection of networks was performed by qualitatively comparing the knock-down experiments with the knock-down in-situ data. This showed that five of the eight found networks matched their Chd expression with the knock-down data. The BMP expression does not appear to be localized to either the oral or aboral side. Of these five networks, only Network 3.6 (see Figure 5.1) showed a low gradient of the BMP expression between the two sides. Therefore, Network 3.6 seems to be the best network capable of replicating both the wild-type and knock-down data of a *Nematostella vectensis* embryo and is thus the most likely candidate to describe the bilateral development of a *Nematostella vectensis* embryo.

A quantitative analysis of the knock-down in-situ data would still need to be performed to verify the validity of Network 3.6 and the other networks. The proposed method keeps the endoderm and ectoderm layers separate, which should give more accurate results.

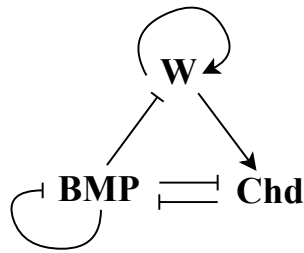


FIGURE 5.1: The gene regulatory network of Network 3.6. This network was able to replicate the asymmetric expression of the wild-type in-situ data and was most in line with the qualitative comparison against the knock-down data. Therefore, Network 3.6 seems to be the most likely candidate to describe the inner workings of the embryo of *Nematostella vectensis*.

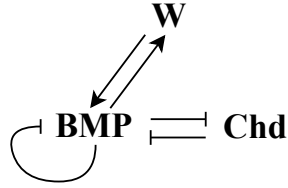
# Appendix A

## Network results

The results of the 16 networks proposed by Oud [\[5\]](#). The results show the parameters after optimization by the EA and the expressions of BMP, Chd and W with and without knock-down experiments. A summary of these results is shown in Table [3.1](#).



## A.1 Network 2.1



$$\sigma_{\text{BMP}} = \bar{\sigma}_{\text{BMP-R} > \text{BMP}} \sigma_{\text{W} > \text{BMP}} \quad (\text{A.1})$$

$$\sigma_{\text{Chd}} = \bar{\sigma}_{\text{BMP-R} > \text{Chd}} \quad (\text{A.2})$$

$$\sigma_{\text{W}} = \sigma_{\text{BMP-R} > \text{W}} \quad (\text{A.3})$$

TABLE A.1: Final parameters of Network 2.1

Parameter	Value	Parameter	Value
$D$	$1.54 \cdot 10^2 \mu\text{m}^2\text{s}^{-1}$	$k_{\text{off}}^{\text{BMP-R}}$	$5.38 \cdot 10^{-8} \text{s}^{-1}$
$\delta_{\text{BMP-R}}$	$3.85 \cdot 10^{-4} \text{s}^{-1}$	$k_{\text{on}}^{\text{BMP-Chd}}$	$7.31 \cdot 10^1 \text{s}^{-1}$
$\delta_{\text{W}}$	$1.63 \cdot 10^{-3} \text{s}^{-1}$	$k_{\text{on}}^{\text{BMP-R}}$	$4.87 \cdot 10^{-1} \text{s}^{-1}$
$K_{\text{BMP-R} > \text{BMP}}$	$2.38 \cdot 10^{-1} \mu\text{M}$	$\rho_{\text{BMP}}$	$8.77 \cdot 10^{-3} \mu\text{Ms}^{-1}$
$K_{\text{BMP-R} > \text{Chd}}$	$2.60 \cdot 10^{-1} \mu\text{M}$	$\rho_{\text{Chd}}$	$3.26 \cdot 10^{-1} \mu\text{Ms}^{-1}$
$K_{\text{BMP-R} > \text{W}}$	$1.07 \cdot 10^{-1} \mu\text{M}$	$\rho_{\text{W}}$	$3.96 \cdot 10^{-2} \mu\text{Ms}^{-1}$
$K_{\text{W} > \text{BMP}}$	$2.58 \cdot 10^{-2} \mu\text{M}$	$R_{\text{tot}}^{\text{BMP}}$	$1.48 \cdot 10^1 \mu\text{M}$
$k_{\text{off}}^{\text{BMP-Chd}}$	$4.10 \cdot 10^{-6} \text{s}^{-1}$	$\tau$	$8.32 \cdot 10^{-2} \text{s}^{-1}$

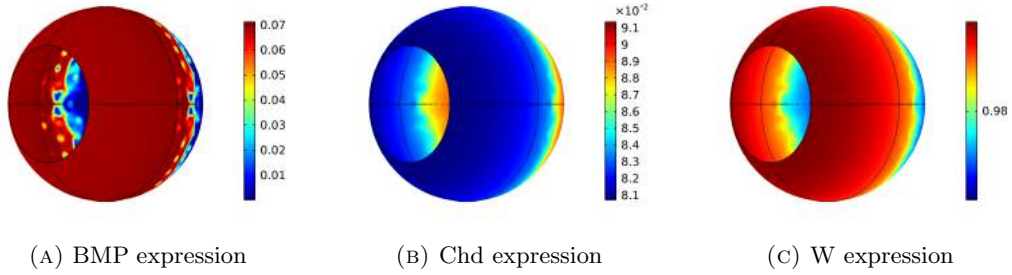


FIGURE A.1: Expression levels of Network 2.1 after parameter optimization.

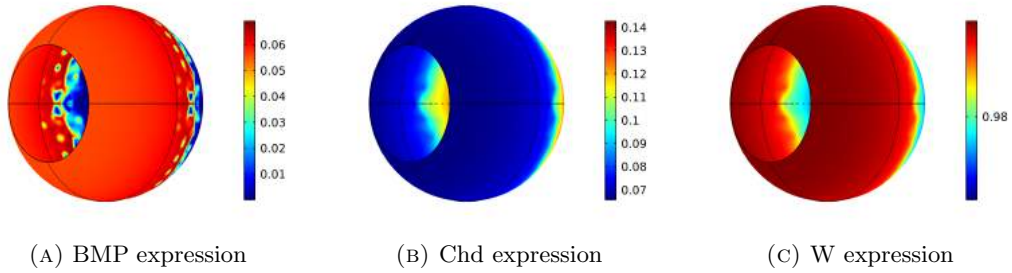
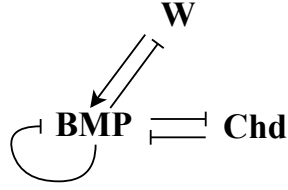


FIGURE A.2: Expression levels of Network 2.1 after Chd knock-out.

## A.2 Network 2.2



$$\sigma_{\text{BMP}} = \bar{\sigma}_{\text{BMP-R} > \text{BMP}} \sigma_{\text{W} > \text{BMP}} \quad (\text{A.4})$$

$$\sigma_{\text{Chd}} = \bar{\sigma}_{\text{BMP-R} > \text{Chd}} \quad (\text{A.5})$$

$$\sigma_{\text{W}} = \bar{\sigma}_{\text{BMP-R} > \text{W}} \quad (\text{A.6})$$

TABLE A.2: Final parameters of Network 2.2

Parameter	Value	Parameter	Value
$D$	$4.50 \cdot 10^1 \mu\text{m}^2\text{s}^{-1}$	$k_{\text{off}}^{\text{BMP-R}}$	$1.63 \cdot 10^{-5} \text{s}^{-1}$
$\delta_{\text{BMP-R}}$	$9.34 \cdot 10^{-4} \text{s}^{-1}$	$k_{\text{on}}^{\text{BMP-Chd}}$	$1.11 \cdot 10^2 \text{s}^{-1}$
$\delta_{\text{W}}$	$4.73 \cdot 10^{-3} \text{s}^{-1}$	$k_{\text{on}}^{\text{BMP-R}}$	$1.19 \cdot 10^0 \text{s}^{-1}$
$K_{\text{BMP-R} > \text{BMP}}$	$2.29 \cdot 10^0 \mu\text{M}$	$\rho_{\text{BMP}}$	$6.36 \cdot 10^{-4} \mu\text{Ms}^{-1}$
$K_{\text{BMP-R} > \text{Chd}}$	$4.19 \cdot 10^{-1} \mu\text{M}$	$\rho_{\text{Chd}}$	$2.79 \cdot 10^{-2} \mu\text{Ms}^{-1}$
$K_{\text{BMP-R} > \text{W}}$	$9.71 \cdot 10^{-2} \mu\text{M}$	$\rho_{\text{W}}$	$2.19 \cdot 10^{-2} \mu\text{Ms}^{-1}$
$K_{\text{W} > \text{BMP}}$	$2.61 \cdot 10^{-2} \mu\text{M}$	$R_{\text{tot}}^{\text{BMP}}$	$1.41 \cdot 10^1 \mu\text{M}$
$k_{\text{off}}^{\text{BMP-Chd}}$	$1.97 \cdot 10^{-6} \text{s}^{-1}$	$\tau$	$6.82 \cdot 10^{-3} \text{s}^{-1}$

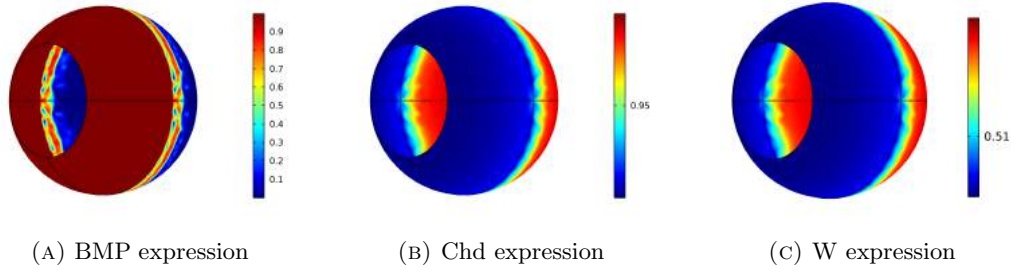


FIGURE A.3: Expression levels of Network 2.2 after parameter optimization.

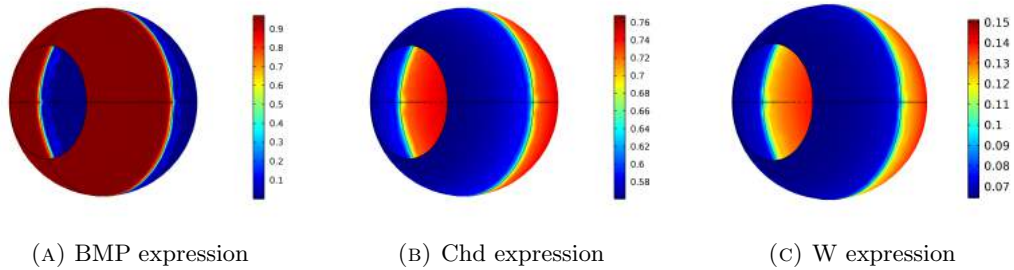
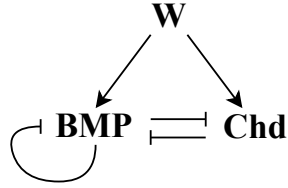


FIGURE A.4: Expression levels of Network 2.2 after Chd knock-out.

### A.3 Network 2.3



$$\sigma_{\text{BMP}} = \bar{\sigma}_{\text{BMP-R} > \text{BMP}} \sigma_{\text{W} > \text{BMP}} \quad (\text{A.7})$$

$$\sigma_{\text{Chd}} = \bar{\sigma}_{\text{BMP-R} > \text{Chd}} \sigma_{\text{W} > \text{Chd}} \quad (\text{A.8})$$

$$\sigma_{\text{W}} = 1 \quad (\text{A.9})$$

TABLE A.3: Final parameters of Network 2.3

Parameter	Value	Parameter	Value
$D$	$2.29 \cdot 10^2 \mu\text{m}^2\text{s}^{-1}$	$k_{\text{off}}^{\text{BMP-R}}$	$3.01 \cdot 10^{-5} \text{s}^{-1}$
$\delta_{\text{BMP-R}}$	$5.40 \cdot 10^{-4} \text{s}^{-1}$	$k_{\text{on}}^{\text{BMP-Chd}}$	$2.10 \cdot 10^2 \text{s}^{-1}$
$\delta_{\text{W}}$	$5.23 \cdot 10^{-5} \text{s}^{-1}$	$k_{\text{on}}^{\text{BMP-R}}$	$1.93 \cdot 10^{-1} \text{s}^{-1}$
$K_{\text{BMP-R} > \text{BMP}}$	$4.52 \cdot 10^{-1} \mu\text{M}$	$\rho_{\text{BMP}}$	$1.16 \cdot 10^{-3} \mu\text{Ms}^{-1}$
$K_{\text{BMP-R} > \text{Chd}}$	$2.81 \cdot 10^{-1} \mu\text{M}$	$\rho_{\text{Chd}}$	$7.79 \cdot 10^{-2} \mu\text{Ms}^{-1}$
$K_{\text{W} > \text{BMP}}$	$2.72 \cdot 10^{-2} \mu\text{M}$	$\rho_{\text{W}}$	$4.86 \cdot 10^{-3} \mu\text{Ms}^{-1}$
$K_{\text{W} > \text{Chd}}$	$1.84 \cdot 10^{-2} \mu\text{M}$	$R_{\text{tot}}^{\text{BMP}}$	$8.86 \cdot 10^{-1} \mu\text{M}$
$k_{\text{off}}^{\text{BMP-Chd}}$	$1.63 \cdot 10^{-6} \text{s}^{-1}$	$\tau$	$8.55 \cdot 10^{-2} \text{s}^{-1}$

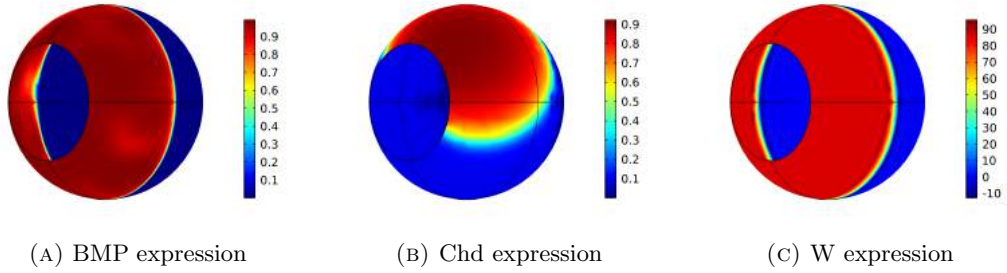


FIGURE A.5: Expression levels of Network 2.3 after parameter optimization.

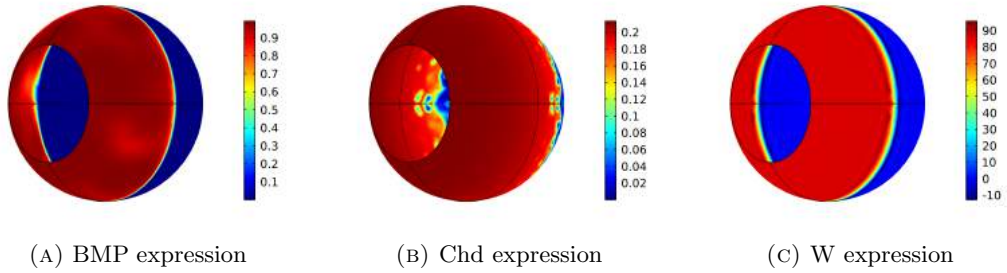
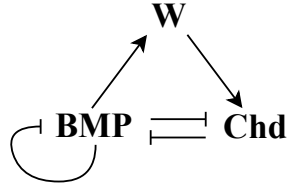


FIGURE A.6: Expression levels of Network 2.3 after Chd knock-out.

## A.4 Network 2.4



$$\sigma_{\text{BMP}} = \bar{\sigma}_{\text{BMP-R} > \text{BMP}} \quad (\text{A.10})$$

$$\sigma_{\text{Chd}} = \bar{\sigma}_{\text{BMP-R} > \text{Chd}} \sigma_{\text{W} > \text{Chd}} \quad (\text{A.11})$$

$$\sigma_{\text{W}} = \sigma_{\text{BMP-R} > \text{W}} \quad (\text{A.12})$$

TABLE A.4: Final parameters of Network 2.4

Parameter	Value	Parameter	Value
$D$	$2.50 \cdot 10^2 \mu\text{m}^2\text{s}^{-1}$	$k_{\text{off}}^{\text{BMP-R}}$	$4.60 \cdot 10^{-6} \text{s}^{-1}$
$\delta_{\text{BMP-R}}$	$3.01 \cdot 10^{-4} \text{s}^{-1}$	$k_{\text{on}}^{\text{BMP-Chd}}$	$8.04 \cdot 10^1 \text{s}^{-1}$
$\delta_{\text{W}}$	$7.45 \cdot 10^{-3} \text{s}^{-1}$	$k_{\text{on}}^{\text{BMP-R}}$	$1.14 \cdot 10^{-1} \text{s}^{-1}$
$K_{\text{BMP-R} > \text{BMP}}$	$6.63 \cdot 10^{-2} \mu\text{M}$	$\rho_{\text{BMP}}$	$1.16 \cdot 10^{-2} \mu\text{Ms}^{-1}$
$K_{\text{BMP-R} > \text{Chd}}$	$3.03 \cdot 10^{-1} \mu\text{M}$	$\rho_{\text{Chd}}$	$8.98 \cdot 10^{-2} \mu\text{Ms}^{-1}$
$K_{\text{BMP-R} > \text{W}}$	$9.99 \cdot 10^{-2} \mu\text{M}$	$\rho_{\text{W}}$	$4.18 \cdot 10^{-3} \mu\text{Ms}^{-1}$
$K_{\text{W} > \text{Chd}}$	$5.66 \cdot 10^{-2} \mu\text{M}$	$R_{\text{tot}}^{\text{BMP}}$	$1.18 \cdot 10^0 \mu\text{M}$
$k_{\text{off}}^{\text{BMP-Chd}}$	$1.67 \cdot 10^{-5} \text{s}^{-1}$	$\tau$	$8.10 \cdot 10^{-2} \text{s}^{-1}$

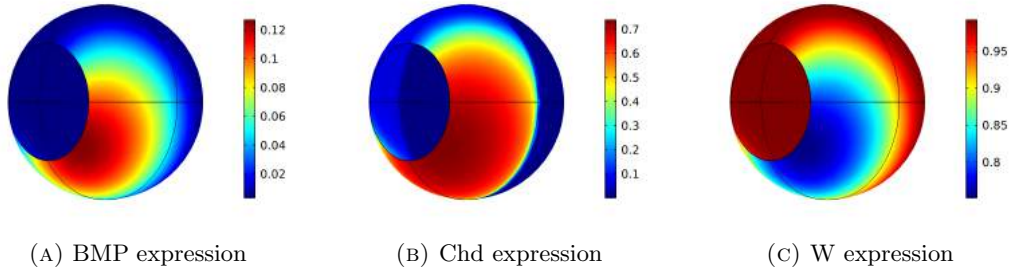


FIGURE A.7: Expression levels of Network 2.4 after parameter optimization.

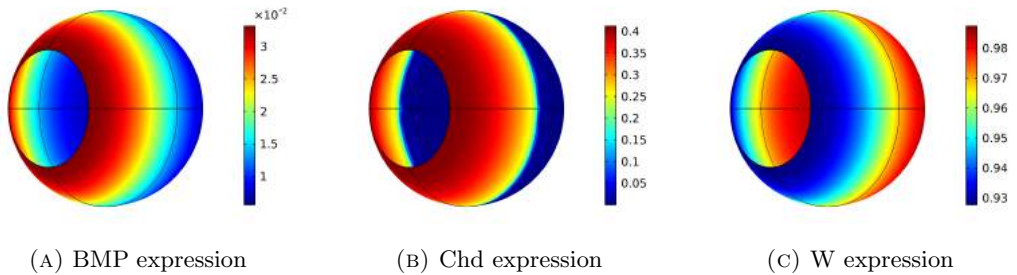
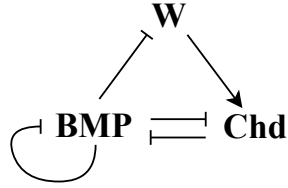


FIGURE A.8: Expression levels of Network 2.4 after Chd knock-out.

## A.5 Network 2.5



$$\sigma_{\text{BMP}} = \bar{\sigma}_{\text{BMP-R} > \text{BMP}} \quad (\text{A.13})$$

$$\sigma_{\text{Chd}} = \bar{\sigma}_{\text{BMP-R} > \text{Chd}} \sigma_{\text{W} > \text{Chd}} \quad (\text{A.14})$$

$$\sigma_{\text{W}} = \bar{\sigma}_{\text{BMP-R} > \text{W}} \quad (\text{A.15})$$

TABLE A.5: Final parameters of Network 2.5

Parameter	Value	Parameter	Value
$D$	$5.44 \cdot 10^2 \mu\text{m}^2\text{s}^{-1}$	$k_{\text{off}}^{\text{BMP-R}}$	$6.11 \cdot 10^{-7} \text{s}^{-1}$
$\delta_{\text{BMP-R}}$	$3.26 \cdot 10^{-3} \text{s}^{-1}$	$k_{\text{on}}^{\text{BMP-Chd}}$	$8.07 \cdot 10^1 \text{s}^{-1}$
$\delta_{\text{W}}$	$3.40 \cdot 10^{-3} \text{s}^{-1}$	$k_{\text{on}}^{\text{BMP-R}}$	$1.02 \cdot 10^0 \text{s}^{-1}$
$K_{\text{BMP-R} > \text{BMP}}$	$6.23 \cdot 10^{-2} \mu\text{M}$	$\rho_{\text{BMP}}$	$1.52 \cdot 10^{-3} \mu\text{Ms}^{-1}$
$K_{\text{BMP-R} > \text{Chd}}$	$1.98 \cdot 10^{-1} \mu\text{M}$	$\rho_{\text{Chd}}$	$1.49 \cdot 10^{-1} \mu\text{Ms}^{-1}$
$K_{\text{BMP-R} > \text{W}}$	$4.81 \cdot 10^{-2} \mu\text{M}$	$\rho_{\text{W}}$	$1.51 \cdot 10^{-3} \mu\text{Ms}^{-1}$
$K_{\text{W} > \text{Chd}}$	$2.67 \cdot 10^{-1} \mu\text{M}$	$R_{\text{tot}}^{\text{BMP}}$	$3.21 \cdot 10^{-1} \mu\text{M}$
$k_{\text{off}}^{\text{BMP-Chd}}$	$5.44 \cdot 10^{-7} \text{s}^{-1}$	$\tau$	$5.78 \cdot 10^{-2} \text{s}^{-1}$

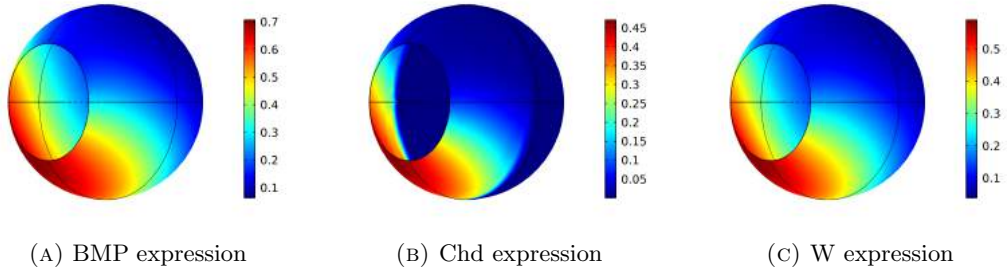


FIGURE A.9: Expression levels of Network 2.5 after parameter optimization.

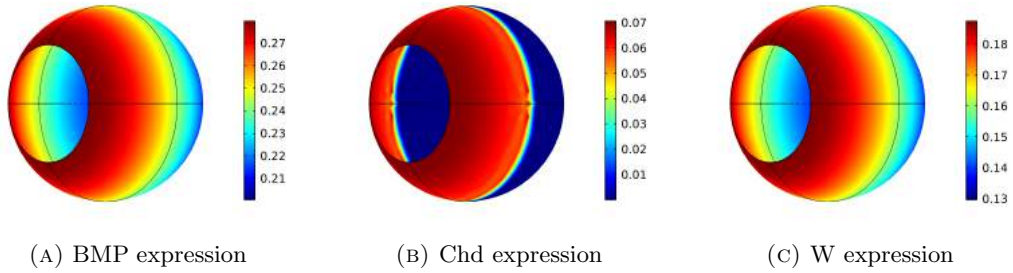
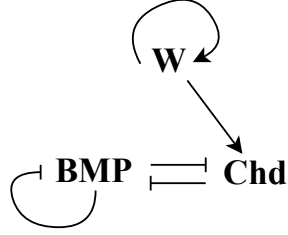


FIGURE A.10: Expression levels of Network 2.5 after Chd knock-out.

## A.6 Network 2.6



$$\sigma_{\text{BMP}} = \bar{\sigma}_{\text{BMP-R} > \text{BMP}} \quad (\text{A.16})$$

$$\sigma_{\text{Chd}} = \bar{\sigma}_{\text{BMP-R} > \text{Chd}} \sigma_{\text{W} > \text{Chd}} \quad (\text{A.17})$$

$$\sigma_{\text{W}} = \sigma_{\text{W} > \text{W}} \quad (\text{A.18})$$

TABLE A.6: Final parameters of Network 2.6

Parameter	Value	Parameter	Value
$D$	$5.15 \cdot 10^1 \mu\text{m}^2\text{s}^{-1}$	$k_{\text{off}}^{\text{BMP-R}}$	$7.42 \cdot 10^{-6} \text{s}^{-1}$
$\delta_{\text{BMP-R}}$	$2.14 \cdot 10^{-4} \text{s}^{-1}$	$k_{\text{on}}^{\text{BMP-Chd}}$	$1.90 \cdot 10^2 \text{s}^{-1}$
$\delta_{\text{W}}$	$3.23 \cdot 10^{-4} \text{s}^{-1}$	$k_{\text{on}}^{\text{BMP-R}}$	$9.31 \cdot 10^{-3} \text{s}^{-1}$
$K_{\text{BMP-R} > \text{BMP}}$	$2.73 \cdot 10^0 \mu\text{M}$	$\rho_{\text{BMP}}$	$8.06 \cdot 10^{-4} \mu\text{Ms}^{-1}$
$K_{\text{BMP-R} > \text{Chd}}$	$2.94 \cdot 10^{-2} \mu\text{M}$	$\rho_{\text{Chd}}$	$1.07 \cdot 10^{-1} \mu\text{Ms}^{-1}$
$K_{\text{W} > \text{Chd}}$	$1.20 \cdot 10^{-2} \mu\text{M}$	$\rho_{\text{W}}$	$7.78 \cdot 10^{-3} \mu\text{Ms}^{-1}$
$K_{\text{W} > \text{W}}$	$2.57 \cdot 10^0 \mu\text{M}$	$R_{\text{tot}}^{\text{BMP}}$	$6.93 \cdot 10^0 \mu\text{M}$
$k_{\text{off}}^{\text{BMP-Chd}}$	$3.39 \cdot 10^{-5} \text{s}^{-1}$	$\tau$	$7.23 \cdot 10^{-2} \text{s}^{-1}$

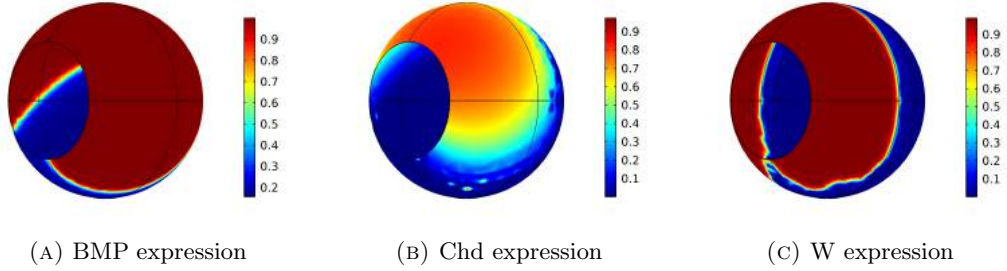


FIGURE A.11: Expression levels of Network 2.6 after parameter optimization.

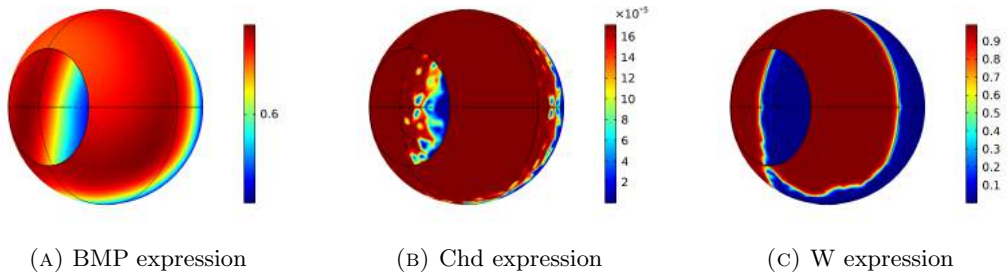
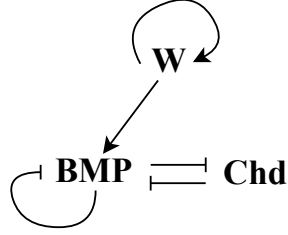


FIGURE A.12: Expression levels of Network 2.6 after Chd knock-out.

## A.7 Network 2.7



$$\sigma_{\text{BMP}} = \bar{\sigma}_{\text{BMP-R} > \text{BMP}} \sigma_{\text{W} > \text{BMP}} \quad (\text{A.19})$$

$$\sigma_{\text{Chd}} = \bar{\sigma}_{\text{BMP-R} > \text{Chd}} \quad (\text{A.20})$$

$$\sigma_{\text{W}} = \sigma_{\text{W} > \text{W}} \quad (\text{A.21})$$

TABLE A.7: Final parameters of Network 2.7

Parameter	Value	Parameter	Value
$D$	$2.52 \cdot 10^2 \quad \mu\text{m}^2\text{s}^{-1}$	$k_{\text{off}}^{\text{BMP-R}}$	$4.24 \cdot 10^{-6} \quad \text{s}^{-1}$
$\delta_{\text{BMP-R}}$	$1.12 \cdot 10^{-3} \quad \text{s}^{-1}$	$k_{\text{on}}^{\text{BMP-Chd}}$	$4.59 \cdot 10^1 \quad \text{s}^{-1}$
$\delta_{\text{W}}$	$1.88 \cdot 10^{-3} \quad \text{s}^{-1}$	$k_{\text{on}}^{\text{BMP-R}}$	$1.18 \cdot 10^0 \quad \text{s}^{-1}$
$K_{\text{BMP-R} > \text{BMP}}$	$3.37 \cdot 10^{-1} \quad \mu\text{M}$	$\rho_{\text{BMP}}$	$1.10 \cdot 10^{-3} \quad \mu\text{Ms}^{-1}$
$K_{\text{BMP-R} > \text{Chd}}$	$1.21 \cdot 10^{-1} \quad \mu\text{M}$	$\rho_{\text{Chd}}$	$1.80 \cdot 10^{-1} \quad \mu\text{Ms}^{-1}$
$K_{\text{W} > \text{BMP}}$	$2.09 \cdot 10^{-2} \quad \mu\text{M}$	$\rho_{\text{W}}$	$2.75 \cdot 10^{-3} \quad \mu\text{Ms}^{-1}$
$K_{\text{W} > \text{W}}$	$3.50 \cdot 10^{-1} \quad \mu\text{M}$	$R_{\text{tot}}^{\text{BMP}}$	$4.38 \cdot 10^0 \quad \mu\text{M}$
$k_{\text{off}}^{\text{BMP-Chd}}$	$5.84 \cdot 10^{-6} \quad \text{s}^{-1}$	$\tau$	$1.26 \cdot 10^{-1} \quad \text{s}^{-1}$

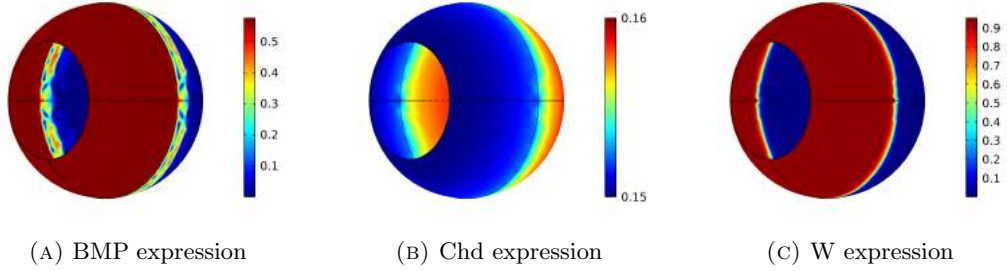


FIGURE A.13: Expression levels of Network 2.7 after parameter optimization.

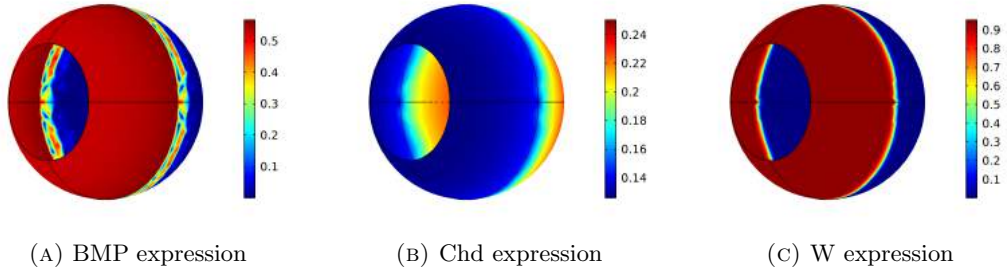
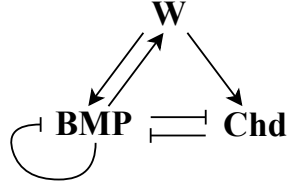


FIGURE A.14: Expression levels of Network 2.7 after Chd knock-out.



## A.8 Network 3.1



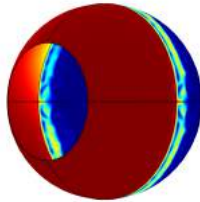
$$\sigma_{\text{BMP}} = \bar{\sigma}_{\text{BMP-R} \rightarrow \text{BMP}} \sigma_{\text{W} \rightarrow \text{BMP}} \quad (\text{A.22})$$

$$\sigma_{\text{Chd}} = \bar{\sigma}_{\text{BMP-R} \rightarrow \text{Chd}} \sigma_{\text{W} \rightarrow \text{Chd}} \quad (\text{A.23})$$

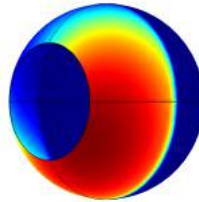
$$\sigma_{\text{W}} = \sigma_{\text{BMP-R} \rightarrow \text{W}} \quad (\text{A.24})$$

TABLE A.8: Final parameters of Network 3.1

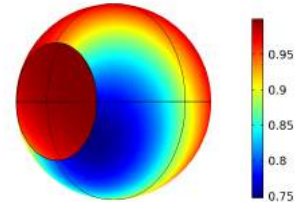
Parameter	Value	Parameter	Value
$D$	$1.28 \cdot 10^2 \mu\text{m}^2\text{s}^{-1}$	$k_{\text{off}}^{\text{BMP-R}}$	$1.14 \cdot 10^{-5} \text{s}^{-1}$
$\delta_{\text{BMP-R}}$	$1.02 \cdot 10^{-3} \text{s}^{-1}$	$k_{\text{on}}^{\text{BMP-Chd}}$	$4.65 \cdot 10^2 \text{s}^{-1}$
$\delta_{\text{W}}$	$3.58 \cdot 10^{-3} \text{s}^{-1}$	$k_{\text{on}}^{\text{BMP-R}}$	$1.88 \cdot 10^{-1} \text{s}^{-1}$
$K_{\text{BMP-R} \rightarrow \text{BMP}}$	$7.09 \cdot 10^{-1} \mu\text{M}$	$\rho_{\text{BMP}}$	$7.48 \cdot 10^{-4} \mu\text{Ms}^{-1}$
$K_{\text{BMP-R} \rightarrow \text{Chd}}$	$5.24 \cdot 10^{-2} \mu\text{M}$	$\rho_{\text{Chd}}$	$9.50 \cdot 10^{-2} \mu\text{Ms}^{-1}$
$K_{\text{BMP-R} \rightarrow \text{W}}$	$2.21 \cdot 10^{-2} \mu\text{M}$	$\rho_{\text{W}}$	$2.38 \cdot 10^{-3} \mu\text{Ms}^{-1}$
$K_{\text{W} \rightarrow \text{BMP}}$	$1.17 \cdot 10^{-2} \mu\text{M}$	$R_{\text{tot}}^{\text{BMP}}$	$8.01 \cdot 10^0 \mu\text{M}$
$K_{\text{W} \rightarrow \text{Chd}}$	$1.85 \cdot 10^{-1} \mu\text{M}$	$\tau$	$7.30 \cdot 10^{-2} \text{s}^{-1}$
$k_{\text{off}}^{\text{BMP-Chd}}$	$9.39 \cdot 10^{-6} \text{s}^{-1}$		



(A) BMP expression

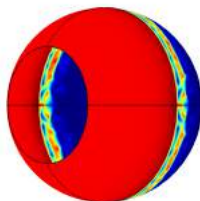


(B) Chd expression

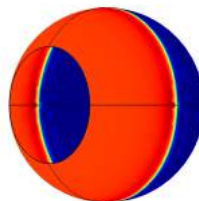


(C) W expression

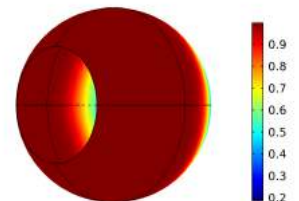
FIGURE A.15: Expression levels of Network 3.1 after parameter optimization.



(A) BMP expression



(B) Chd expression

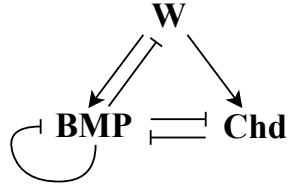


(C) W expression

FIGURE A.16: Expression levels of Network 3.1 after Chd knock-out.



## A.9 Network 3.2



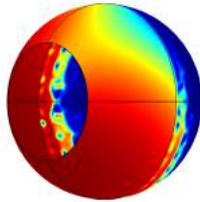
$$\sigma_{\text{BMP}} = \bar{\sigma}_{\text{BMP-R} > \text{BMP}} \sigma_{\text{W} > \text{BMP}} \quad (\text{A.25})$$

$$\sigma_{\text{Chd}} = \bar{\sigma}_{\text{BMP-R} > \text{Chd}} \sigma_{\text{W} > \text{Chd}} \quad (\text{A.26})$$

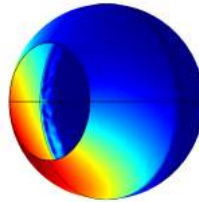
$$\sigma_{\text{W}} = \sigma_{\text{BMP-R} > \text{W}} \quad (\text{A.27})$$

TABLE A.9: Final parameters of Network 3.2

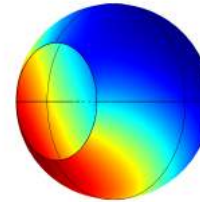
Parameter	Value	Parameter	Value
$D$	$1.15 \cdot 10^2 \quad \mu\text{m}^2\text{s}^{-1}$	$k_{\text{off}}^{\text{BMP-R}}$	$9.96 \cdot 10^{-6} \quad \text{s}^{-1}$
$\delta_{\text{BMP-R}}$	$5.89 \cdot 10^{-4} \quad \text{s}^{-1}$	$k_{\text{on}}^{\text{BMP-Chd}}$	$9.61 \cdot 10^1 \quad \text{s}^{-1}$
$\delta_{\text{W}}$	$1.14 \cdot 10^{-3} \quad \text{s}^{-1}$	$k_{\text{on}}^{\text{BMP-R}}$	$1.29 \cdot 10^{-1} \quad \text{s}^{-1}$
$K_{\text{BMP-R} > \text{BMP}}$	$9.48 \cdot 10^{-1} \quad \mu\text{M}$	$\rho_{\text{BMP}}$	$8.36 \cdot 10^{-4} \quad \mu\text{Ms}^{-1}$
$K_{\text{BMP-R} > \text{Chd}}$	$1.19 \cdot 10^{-1} \quad \mu\text{M}$	$\rho_{\text{Chd}}$	$1.73 \cdot 10^{-1} \quad \mu\text{Ms}^{-1}$
$K_{\text{BMP-R} > \text{W}}$	$2.10 \cdot 10^{-1} \quad \mu\text{M}$	$\rho_{\text{W}}$	$1.15 \cdot 10^{-2} \quad \mu\text{Ms}^{-1}$
$K_{\text{W} > \text{BMP}}$	$1.24 \cdot 10^{-2} \quad \mu\text{M}$	$R_{\text{tot}}^{\text{BMP}}$	$5.70 \cdot 10^0 \quad \mu\text{M}$
$K_{\text{W} > \text{Chd}}$	$1.14 \cdot 10^{-1} \quad \mu\text{M}$	$\tau$	$9.87 \cdot 10^{-2} \quad \text{s}^{-1}$
$k_{\text{off}}^{\text{BMP-Chd}}$	$9.12 \cdot 10^{-7} \quad \text{s}^{-1}$		



(A) BMP expression

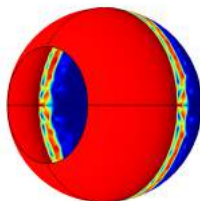


(B) Chd expression

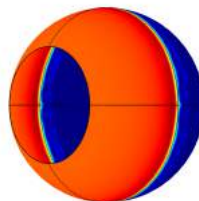


(C) W expression

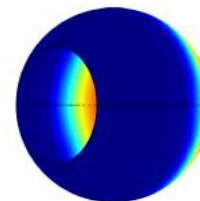
FIGURE A.17: Expression levels of Network 3.2 after parameter optimization.



(A) BMP expression



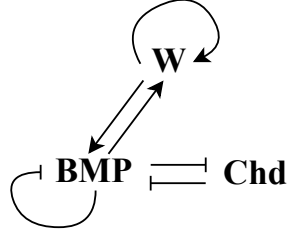
(B) Chd expression



(C) W expression

FIGURE A.18: Expression levels of Network 3.2 after Chd knock-out.

### A.10 Network 3.3



$$\sigma_{\text{BMP}} = \bar{\sigma}_{\text{BMP-R} > \text{BMP}} \sigma_{\text{W} > \text{BMP}} \quad (\text{A.28})$$

$$\sigma_{\text{Chd}} = \bar{\sigma}_{\text{BMP-R} > \text{Chd}} \quad (\text{A.29})$$

$$\sigma_{\text{W}} = \sigma_{\text{BMP-R} > \text{W}} \sigma_{\text{W} > \text{W}} \quad (\text{A.30})$$

TABLE A.10: Final parameters of Network 3.3

Parameter	Value	Parameter	Value
$D$	$1.22 \cdot 10^2 \mu\text{m}^2\text{s}^{-1}$	$k_{\text{off}}^{\text{BMP-R}}$	$1.08 \cdot 10^{-5} \text{s}^{-1}$
$\delta_{\text{BMP-R}}$	$3.94 \cdot 10^{-4} \text{s}^{-1}$	$k_{\text{on}}^{\text{BMP-Chd}}$	$1.58 \cdot 10^2 \text{s}^{-1}$
$\delta_{\text{W}}$	$1.12 \cdot 10^{-3} \text{s}^{-1}$	$k_{\text{on}}^{\text{BMP-R}}$	$2.17 \cdot 10^{-1} \text{s}^{-1}$
$K_{\text{BMP-R} > \text{BMP}}$	$2.49 \cdot 10^{-1} \mu\text{M}$	$\rho_{\text{BMP}}$	$1.82 \cdot 10^{-3} \mu\text{Ms}^{-1}$
$K_{\text{BMP-R} > \text{Chd}}$	$2.79 \cdot 10^{-1} \mu\text{M}$	$\rho_{\text{Chd}}$	$1.08 \cdot 10^{-1} \mu\text{Ms}^{-1}$
$K_{\text{BMP-R} > \text{W}}$	$2.43 \cdot 10^{-3} \mu\text{M}$	$\rho_{\text{W}}$	$2.60 \cdot 10^{-3} \mu\text{Ms}^{-1}$
$K_{\text{W} > \text{BMP}}$	$1.08 \cdot 10^{-3} \mu\text{M}$	$R_{\text{tot}}^{\text{BMP}}$	$1.02 \cdot 10^0 \mu\text{M}$
$K_{\text{W} > \text{W}}$	$4.20 \cdot 10^{-1} \mu\text{M}$	$\tau$	$1.63 \cdot 10^{-1} \text{s}^{-1}$
$k_{\text{off}}^{\text{BMP-Chd}}$	$7.33 \cdot 10^{-6} \text{s}^{-1}$		

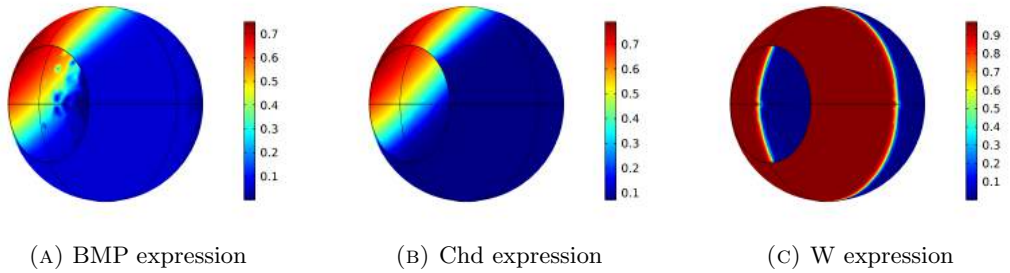


FIGURE A.19: Expression levels of Network 3.3 after parameter optimization.

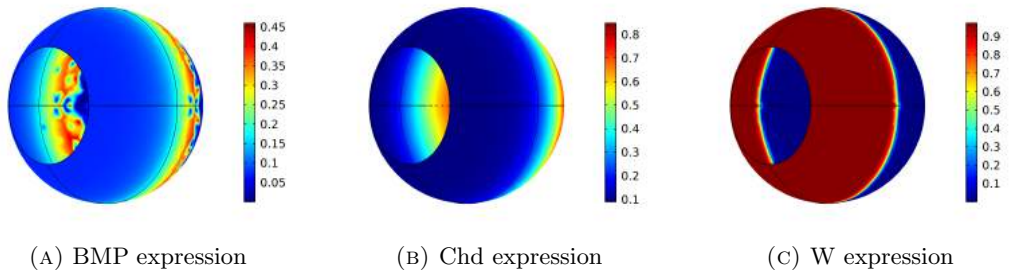
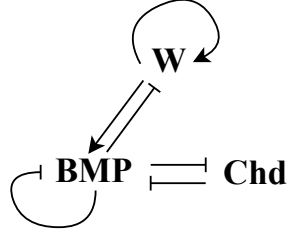


FIGURE A.20: Expression levels of Network 3.3 after Chd knock-out.

### A.11 Network 3.4



$$\sigma_{\text{BMP}} = \bar{\sigma}_{\text{BMP-R} > \text{BMP}} \sigma_{\text{W} > \text{BMP}} \quad (\text{A.31})$$

$$\sigma_{\text{Chd}} = \bar{\sigma}_{\text{BMP-R} > \text{Chd}} \quad (\text{A.32})$$

$$\sigma_{\text{W}} = \bar{\sigma}_{\text{BMP-R} > \text{W}} \sigma_{\text{W} > \text{W}} \quad (\text{A.33})$$

TABLE A.11: Final parameters of Network 3.4

Parameter	Value	Parameter	Value
$D$	$2.28 \cdot 10^1 \mu\text{m}^2\text{s}^{-1}$	$k_{\text{off}}^{\text{BMP-R}}$	$2.06 \cdot 10^{-5} \text{s}^{-1}$
$\delta_{\text{BMP-R}}$	$1.95 \cdot 10^{-4} \text{s}^{-1}$	$k_{\text{on}}^{\text{BMP-Chd}}$	$8.38 \cdot 10^2 \text{s}^{-1}$
$\delta_{\text{W}}$	$4.43 \cdot 10^0 \text{s}^{-1}$	$k_{\text{on}}^{\text{BMP-R}}$	$1.12 \cdot 10^{-1} \text{s}^{-1}$
$K_{\text{BMP-R} > \text{BMP}}$	$8.72 \cdot 10^{-4} \mu\text{M}$	$\rho_{\text{BMP}}$	$6.31 \cdot 10^{-4} \mu\text{Ms}^{-1}$
$K_{\text{BMP-R} > \text{Chd}}$	$2.08 \cdot 10^{-2} \mu\text{M}$	$\rho_{\text{Chd}}$	$4.16 \cdot 10^{-1} \mu\text{Ms}^{-1}$
$K_{\text{BMP-R} > \text{W}}$	$1.09 \cdot 10^{-3} \mu\text{M}$	$\rho_{\text{W}}$	$3.49 \cdot 10^{-3} \mu\text{Ms}^{-1}$
$K_{\text{W} > \text{BMP}}$	$3.59 \cdot 10^{-2} \mu\text{M}$	$R_{\text{tot}}^{\text{BMP}}$	$3.76 \cdot 10^0 \mu\text{M}$
$K_{\text{W} > \text{W}}$	$4.07 \cdot 10^{-1} \mu\text{M}$	$\tau$	$6.46 \cdot 10^{-2} \text{s}^{-1}$
$k_{\text{off}}^{\text{BMP-Chd}}$	$3.87 \cdot 10^{-5} \text{s}^{-1}$		

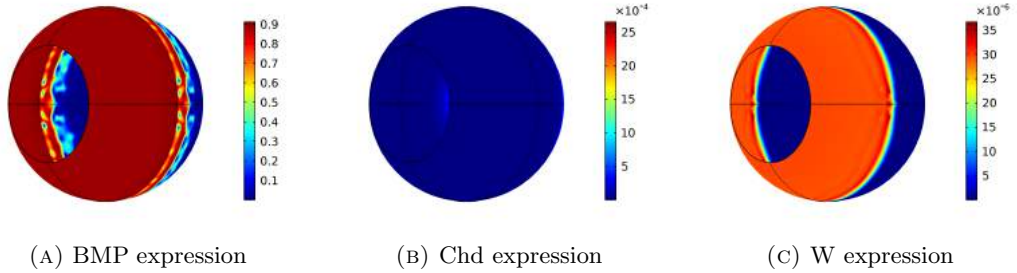


FIGURE A.21: Expression levels of Network 3.4 after parameter optimization.

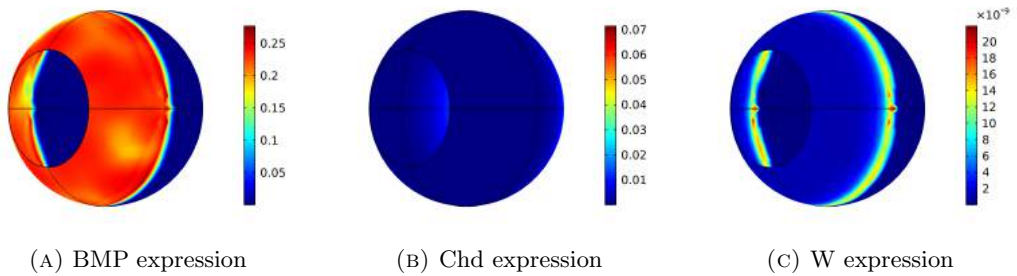
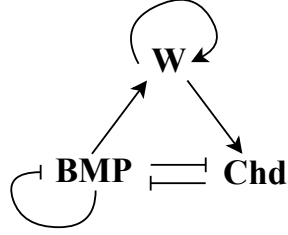


FIGURE A.22: Expression levels of Network 3.4 after Chd knock-out.

## A.12 Network 3.5



$$\sigma_{\text{BMP}} = \bar{\sigma}_{\text{BMP-R} > \text{BMP}} \quad (\text{A.34})$$

$$\sigma_{\text{Chd}} = \bar{\sigma}_{\text{BMP-R} > \text{Chd}} \sigma_{\text{W} > \text{Chd}} \quad (\text{A.35})$$

$$\sigma_{\text{W}} = \sigma_{\text{BMP-R} > \text{W}} \sigma_{\text{W} > \text{W}} \quad (\text{A.36})$$

TABLE A.12: Final parameters of Network 3.5

Parameter	Value	Parameter	Value
$D$	$6.30 \cdot 10^2 \mu\text{m}^2\text{s}^{-1}$	$k_{\text{off}}^{\text{BMP-R}}$	$1.07 \cdot 10^{-6} \text{s}^{-1}$
$\delta_{\text{BMP-R}}$	$5.67 \cdot 10^{-4} \text{s}^{-1}$	$k_{\text{on}}^{\text{BMP-Chd}}$	$6.15 \cdot 10^2 \text{s}^{-1}$
$\delta_{\text{W}}$	$1.25 \cdot 10^{-3} \text{s}^{-1}$	$k_{\text{on}}^{\text{BMP-R}}$	$3.92 \cdot 10^{-1} \text{s}^{-1}$
$K_{\text{BMP-R} > \text{BMP}}$	$9.96 \cdot 10^{-2} \mu\text{M}$	$\rho_{\text{BMP}}$	$1.48 \cdot 10^{-3} \mu\text{Ms}^{-1}$
$K_{\text{BMP-R} > \text{Chd}}$	$4.16 \cdot 10^{-2} \mu\text{M}$	$\rho_{\text{Chd}}$	$3.07 \cdot 10^{-1} \mu\text{Ms}^{-1}$
$K_{\text{BMP-R} > \text{W}}$	$5.71 \cdot 10^{-2} \mu\text{M}$	$\rho_{\text{W}}$	$3.98 \cdot 10^{-3} \mu\text{Ms}^{-1}$
$K_{\text{W} > \text{Chd}}$	$7.71 \cdot 10^{-1} \mu\text{M}$	$R_{\text{tot}}^{\text{BMP}}$	$5.95 \cdot 10^{-1} \mu\text{M}$
$K_{\text{W} > \text{W}}$	$5.50 \cdot 10^{-1} \mu\text{M}$	$\tau$	$1.66 \cdot 10^{-1} \text{s}^{-1}$
$k_{\text{off}}^{\text{BMP-Chd}}$	$2.48 \cdot 10^{-5} \text{s}^{-1}$		

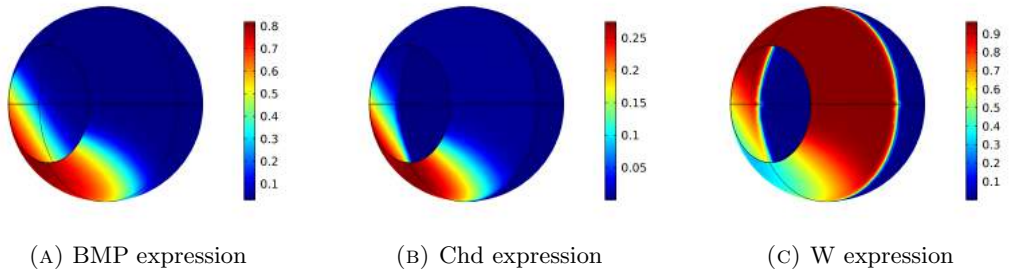


FIGURE A.23: Expression levels of Network 3.5 after parameter optimization.

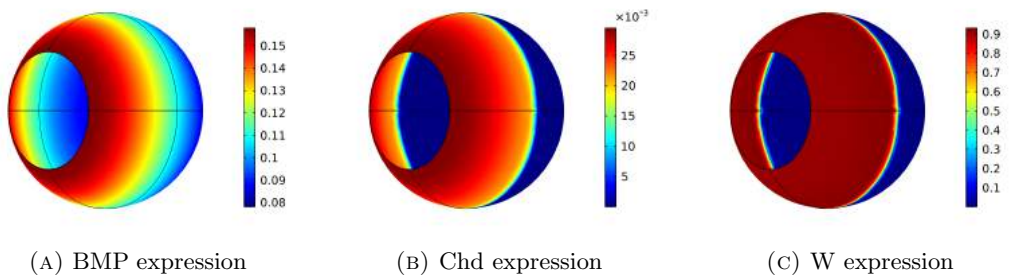
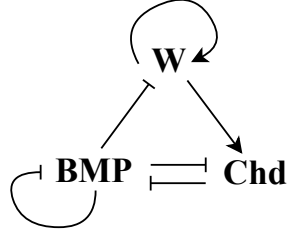


FIGURE A.24: Expression levels of Network 3.5 after Chd knock-out.

### A.13 Network 3.6



$$\sigma_{\text{BMP}} = \bar{\sigma}_{\text{BMP-R} > \text{BMP}} \quad (\text{A.37})$$

$$\sigma_{\text{Chd}} = \bar{\sigma}_{\text{BMP-R} > \text{Chd}} \sigma_{\text{W} > \text{Chd}} \quad (\text{A.38})$$

$$\sigma_{\text{W}} = \sigma_{\text{BMP-R} > \text{W}} \sigma_{\text{W} > \text{W}} \quad (\text{A.39})$$

TABLE A.13: Final parameters of Network 3.6

Parameter	Value	Parameter	Value
$D$	$5.63 \cdot 10^2 \mu\text{m}^2\text{s}^{-1}$	$k_{\text{off}}^{\text{BMP-R}}$	$3.25 \cdot 10^{-5} \text{s}^{-1}$
$\delta_{\text{BMP-R}}$	$4.55 \cdot 10^{-4} \text{s}^{-1}$	$k_{\text{on}}^{\text{BMP-Chd}}$	$3.11 \cdot 10^2 \text{s}^{-1}$
$\delta_{\text{W}}$	$5.16 \cdot 10^{-4} \text{s}^{-1}$	$k_{\text{on}}^{\text{BMP-R}}$	$9.70 \cdot 10^{-2} \text{s}^{-1}$
$K_{\text{BMP-R} > \text{BMP}}$	$3.40 \cdot 10^{-1} \mu\text{M}$	$\rho_{\text{BMP}}$	$1.22 \cdot 10^{-3} \mu\text{Ms}^{-1}$
$K_{\text{BMP-R} > \text{Chd}}$	$1.76 \cdot 10^{-1} \mu\text{M}$	$\rho_{\text{Chd}}$	$1.13 \cdot 10^{-1} \mu\text{Ms}^{-1}$
$K_{\text{BMP-R} > \text{W}}$	$3.91 \cdot 10^{-2} \mu\text{M}$	$\rho_{\text{W}}$	$3.61 \cdot 10^{-3} \mu\text{Ms}^{-1}$
$K_{\text{W} > \text{Chd}}$	$1.03 \cdot 10^{-1} \mu\text{M}$	$R_{\text{tot}}^{\text{BMP}}$	$1.03 \cdot 10^0 \mu\text{M}$
$K_{\text{W} > \text{W}}$	$1.16 \cdot 10^0 \mu\text{M}$	$\tau$	$5.35 \cdot 10^{-1} \text{s}^{-1}$
$k_{\text{off}}^{\text{BMP-Chd}}$	$1.13 \cdot 10^{-5} \text{s}^{-1}$		

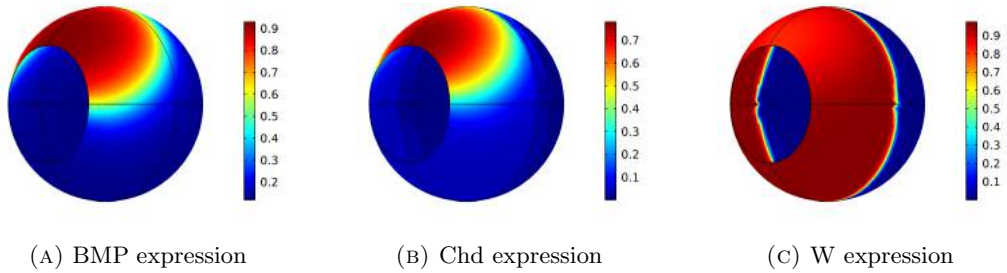


FIGURE A.25: Expression levels of Network 3.6 after parameter optimization.

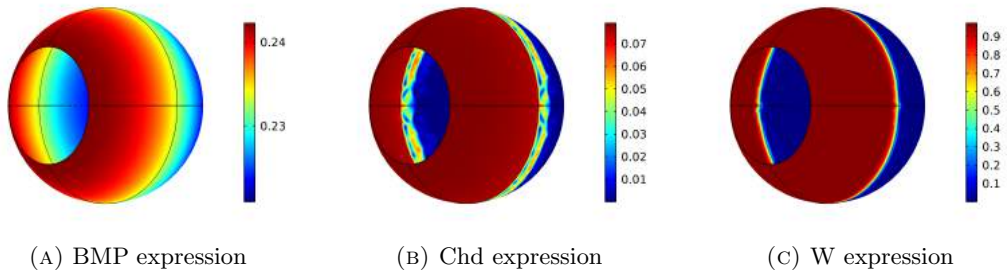
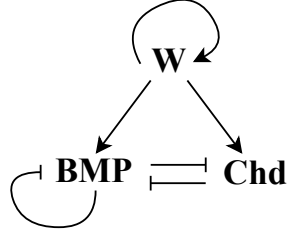


FIGURE A.26: Expression levels of Network 3.6 after Chd knock-out.

## A.14 Network 3.7



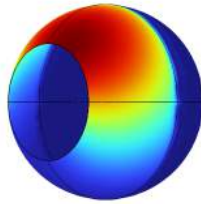
$$\sigma_{\text{BMP}} = \bar{\sigma}_{\text{BMP-R} > \text{BMP}} \sigma_{\text{W} > \text{BMP}} \quad (\text{A.40})$$

$$\sigma_{\text{Chd}} = \bar{\sigma}_{\text{BMP-R} > \text{Chd}} \sigma_{\text{W} > \text{Chd}} \quad (\text{A.41})$$

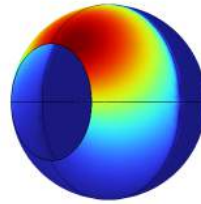
$$\sigma_{\text{W}} = \sigma_{\text{W} > \text{W}} \quad (\text{A.42})$$

TABLE A.14: Final parameters of Network 3.7

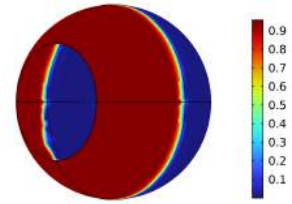
Parameter	Value	Parameter	Value
$D$	$1.48 \cdot 10^2 \mu\text{m}^2\text{s}^{-1}$	$k_{\text{off}}^{\text{BMP-R}}$	$1.05 \cdot 10^{-5} \text{s}^{-1}$
$\delta_{\text{BMP-R}}$	$9.44 \cdot 10^{-5} \text{s}^{-1}$	$k_{\text{on}}^{\text{BMP-Chd}}$	$1.35 \cdot 10^2 \text{s}^{-1}$
$\delta_{\text{W}}$	$1.06 \cdot 10^{-3} \text{s}^{-1}$	$k_{\text{on}}^{\text{BMP-R}}$	$1.14 \cdot 10^{-1} \text{s}^{-1}$
$K_{\text{BMP-R} > \text{BMP}}$	$5.77 \cdot 10^{-1} \mu\text{M}$	$\rho_{\text{BMP}}$	$2.53 \cdot 10^{-3} \mu\text{Ms}^{-1}$
$K_{\text{BMP-R} > \text{Chd}}$	$2.69 \cdot 10^{-1} \mu\text{M}$	$\rho_{\text{Chd}}$	$4.67 \cdot 10^{-1} \mu\text{Ms}^{-1}$
$K_{\text{W} > \text{BMP}}$	$4.17 \cdot 10^{-1} \mu\text{M}$	$\rho_{\text{W}}$	$4.90 \cdot 10^{-3} \mu\text{Ms}^{-1}$
$K_{\text{W} > \text{Chd}}$	$6.54 \cdot 10^{-1} \mu\text{M}$	$R_{\text{tot}}^{\text{BMP}}$	$7.30 \cdot 10^0 \mu\text{M}$
$K_{\text{W} > \text{W}}$	$1.10 \cdot 10^0 \mu\text{M}$	$\tau$	$2.61 \cdot 10^{-2} \text{s}^{-1}$
$k_{\text{off}}^{\text{BMP-Chd}}$	$1.08 \cdot 10^{-6} \text{s}^{-1}$		



(A) BMP expression

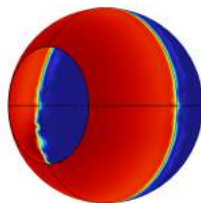


(B) Chd expression

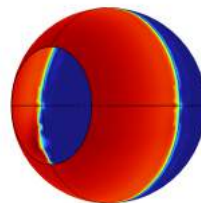


(C) W expression

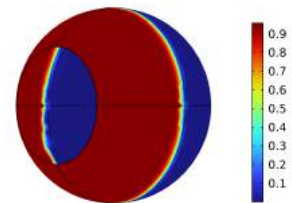
FIGURE A.27: Expression levels of Network 3.7 after parameter optimization.



(A) BMP expression



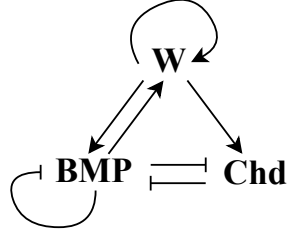
(B) Chd expression



(C) W expression

FIGURE A.28: Expression levels of Network 3.7 after Chd knock-out.

## A.15 Network 4.1



$$\sigma_{\text{BMP}} = \bar{\sigma}_{\text{BMP-R} > \text{BMP}} \sigma_{\text{W} > \text{BMP}} \quad (\text{A.43})$$

$$\sigma_{\text{Chd}} = \bar{\sigma}_{\text{BMP-R} > \text{Chd}} \sigma_{\text{W} > \text{Chd}} \quad (\text{A.44})$$

$$\sigma_{\text{W}} = \sigma_{\text{BMP-R} > \text{W}} \sigma_{\text{W} > \text{W}} \quad (\text{A.45})$$

TABLE A.15: Final parameters of Network 4.1

Parameter	Value	Parameter	Value
$D$	$6.68 \cdot 10^1 \mu\text{m}^2\text{s}^{-1}$	$k_{\text{off}}^{\text{BMP-Chd}}$	$2.71 \cdot 10^{-6} \text{s}^{-1}$
$\delta_{\text{BMP-R}}$	$1.89 \cdot 10^{-4} \text{s}^{-1}$	$k_{\text{off}}^{\text{BMP-R}}$	$1.43 \cdot 10^{-6} \text{s}^{-1}$
$\delta_{\text{W}}$	$4.06 \cdot 10^{-4} \text{s}^{-1}$	$k_{\text{on}}^{\text{BMP-Chd}}$	$5.40 \cdot 10^1 \text{s}^{-1}$
$K_{\text{BMP-R} > \text{BMP}}$	$2.25 \cdot 10^{-1} \mu\text{M}$	$k_{\text{on}}^{\text{BMP-R}}$	$1.87 \cdot 10^{-2} \text{s}^{-1}$
$K_{\text{BMP-R} > \text{Chd}}$	$2.21 \cdot 10^{-1} \mu\text{M}$	$\rho_{\text{BMP}}$	$1.31 \cdot 10^{-3} \mu\text{Ms}^{-1}$
$K_{\text{BMP-R} > \text{W}}$	$8.17 \cdot 10^{-2} \mu\text{M}$	$\rho_{\text{Chd}}$	$7.81 \cdot 10^{-2} \mu\text{Ms}^{-1}$
$K_{\text{W} > \text{BMP}}$	$6.11 \cdot 10^{-2} \mu\text{M}$	$\rho_{\text{W}}$	$3.80 \cdot 10^{-3} \mu\text{Ms}^{-1}$
$K_{\text{W} > \text{Chd}}$	$8.07 \cdot 10^{-2} \mu\text{M}$	$R_{\text{tot}}^{\text{BMP}}$	$1.68 \cdot 10^0 \mu\text{M}$
$K_{\text{W} > \text{W}}$	$3.56 \cdot 10^{-1} \mu\text{M}$	$\tau$	$9.41 \cdot 10^{-2} \text{s}^{-1}$

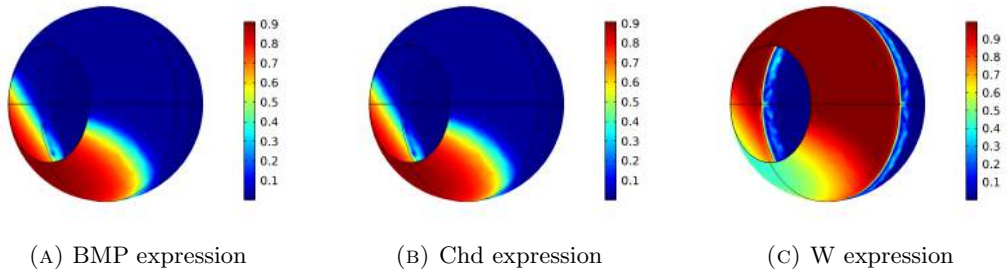


FIGURE A.29: Expression levels of Network 4.1 after parameter optimization.

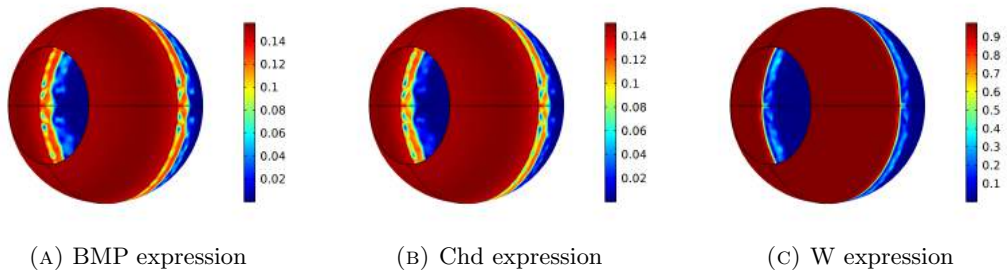
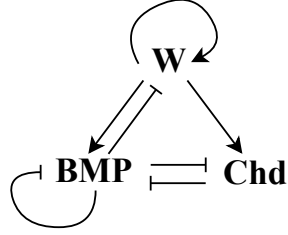


FIGURE A.30: Expression levels of Network 4.1 after Chd knock-out.



## A.16 Network 4.2



$$\sigma_{\text{BMP}} = \bar{\sigma}_{\text{BMP-R} > \text{BMP}} \sigma_{\text{W} > \text{BMP}} \quad (\text{A.46})$$

$$\sigma_{\text{Chd}} = \bar{\sigma}_{\text{BMP-R} > \text{Chd}} \sigma_{\text{W} > \text{Chd}} \quad (\text{A.47})$$

$$\sigma_{\text{W}} = \bar{\sigma}_{\text{BMP-R} > \text{W}} \sigma_{\text{W} > \text{W}} \quad (\text{A.48})$$

TABLE A.16: Final parameters of Network 4.2

Parameter	Value	Parameter	Value
$D$	$4.77 \cdot 10^1 \mu\text{m}^2\text{s}^{-1}$	$k_{\text{off}}^{\text{BMP-Chd}}$	$2.89 \cdot 10^{-6} \text{s}^{-1}$
$\delta_{\text{BMP-R}}$	$4.36 \cdot 10^{-4} \text{s}^{-1}$	$k_{\text{off}}^{\text{BMP-R}}$	$6.24 \cdot 10^{-7} \text{s}^{-1}$
$\delta_{\text{W}}$	$1.02 \cdot 10^{-3} \text{s}^{-1}$	$k_{\text{on}}^{\text{BMP-Chd}}$	$4.05 \cdot 10^1 \text{s}^{-1}$
$K_{\text{BMP-R} > \text{BMP}}$	$2.61 \cdot 10^{-1} \mu\text{M}$	$k_{\text{on}}^{\text{BMP-R}}$	$7.73 \cdot 10^{-2} \text{s}^{-1}$
$K_{\text{BMP-R} > \text{Chd}}$	$1.74 \cdot 10^{-1} \mu\text{M}$	$\rho_{\text{BMP}}$	$1.43 \cdot 10^{-3} \mu\text{Ms}^{-1}$
$K_{\text{BMP-R} > \text{W}}$	$2.91 \cdot 10^{-1} \mu\text{M}$	$\rho_{\text{Chd}}$	$6.05 \cdot 10^{-2} \mu\text{Ms}^{-1}$
$K_{\text{W} > \text{BMP}}$	$2.89 \cdot 10^{-2} \mu\text{M}$	$\rho_{\text{W}}$	$2.58 \cdot 10^{-3} \mu\text{Ms}^{-1}$
$K_{\text{W} > \text{Chd}}$	$1.33 \cdot 10^{-1} \mu\text{M}$	$R_{\text{tot}}^{\text{BMP}}$	$4.92 \cdot 10^{-1} \mu\text{M}$
$K_{\text{W} > \text{W}}$	$4.77 \cdot 10^{-1} \mu\text{M}$	$\tau$	$8.00 \cdot 10^{-2} \text{s}^{-1}$

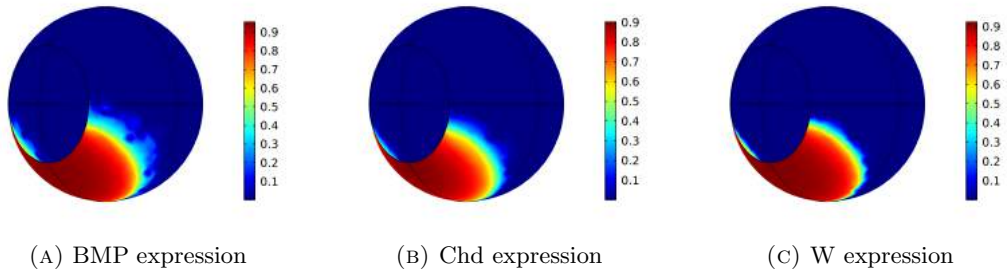


FIGURE A.31: Expression levels of Network 4.2 after parameter optimization.

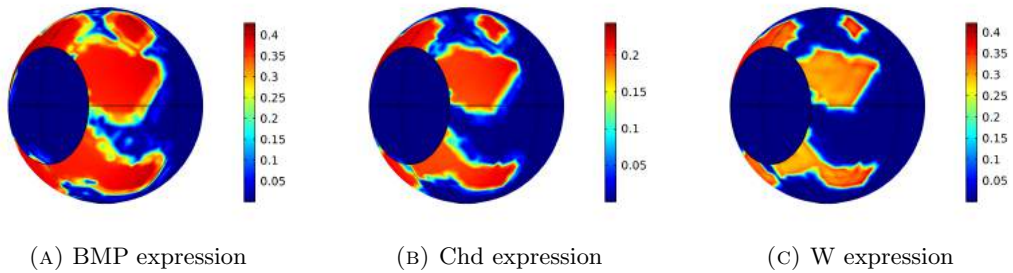


FIGURE A.32: Expression levels of Network 4.2 after Chd knock-out.



## Appendix B

# Project documentation

A program, which runs the EA and DS method, was developed specifically with COMSOL in mind. The EA is designed to run each generation as a COMSOL batchjob. This minimizes the number of COMSOL calls, which would have been a significant computational cost. The EA can be tweaked through several methods. The evaluation, initialization, recombination, and mutations steps of the EA can all be configured. A short description of each file/directory is shown in Table [B.1](#).

Table B.1: A short description of each file and directory used to run the EA and DS method.

File	Description
COMSOL_output/	An empty directory. This directory is filled with the results from the COMSOL batchjob.
ea_options/errors.py	Contains several error functions, such as root mean square error and relative squared error.
ea_options/evaluations.py	Contains several evaluation functions. Some functions are used to test the EA. These will not call COMSOL and are therefore much quicker.
ea_options/initializations.py	Contains several initialization functions.
ea_options/mutations.py	Contains several mutation functions.
ea_options/recombination.py	Contains several recombination functions.
gene_expression/	Contains the processed in-situ data obtained by Greuell.

Continued on next page

Table B.1: A short description of each file and directory used to run the EA and DS method. (Continued)

File	Description
<code>networks/</code>	Contains the available networks. These networks are originally from Oud, but were optimized to improve the performance of the networks.
<code>results/</code>	Contains all the figures and data for each network.
<code>temp/</code>	A temporary directory, which stores intermediate results of the EA. This allows the EA to continue in case the program has prematurely terminated.
<code>agent.py</code>	This class holds the information tied to an instance of each generation. Furthermore, it provides functionality to save the parameters in COMSOL format or as a $\text{\LaTeX}$ table.
<code>best_agent_runner.py</code>	This file runs the best agent of each network. This is used to create the final expression figures and their parameter tables.
<code>comsol_ea.py</code>	This file contains the EA. The EA can start a new run or continue with a previous run. The results from the <code>temp/</code> directory will then be used.
<code>comsol_IO.py</code>	Contains several utility functions related to the input and output from COMSOL.
<code>comsol_output_reader.py</code>	Contains the functionality to parse the 3D mesh data into the linearized expressions. This was originally developed by Greuell.
<code>configurations.py</code>	Contains a set of configurations for each network. The initial parameter values are from Oud.
<code>data_reader.py</code>	Reads the data generated by <code>comsol_ea.py</code> .
<code>data_visualiser.py</code>	Creates several visualisations from the data obtained by <code>data_reader.py</code> .

Continued on next page

Table B.1: A short description of each file and directory used to run the EA and DS method. (Continued)

File	Description
<code>downhill_simplex.py</code>	The implemantation of the DS method. The initial simplex is obtained from the best-performing agents during the EA.
<code>hall_of_fame.py</code>	Keeps track of the best-performing agents during the EA.
<code>knock_out_experiment.py</code>	Runs the knock-down experiments.
<code>logger.py</code>	A logger object, which creates better looking output in the terminal.
<code>reader_utilities.py</code>	A set of utility functions used by <code>comsol_output_reader.py</code> . This was originally developed by Greuell.

# Bibliography

- [1] The UniProt Consortium. Uniprot: the universal protein knowledgebase in 2023. <https://www.uniprot.org/proteomes/UP000001593>, 2023.
- [2] Shuonan He, Florencia Del Viso, Cheng-Yi Chen, Aissam Ikmi, Amanda E Kroesen, and Matthew C Gibson. An axial hox code controls tissue segmentation and body patterning in *nematostella vectensis*. *Science*, 361(6409):1377–1380, 2018.
- [3] Grigory Genikhovich, Patrick Fried, M Mandela Prünster, Johannes B Schinko, Anna F Gilles, David Fredman, Karin Meier, Dagmar Iber, and Ulrich Technau. Axis patterning by bmps: cnidarian network reveals evolutionary constraints. *Cell reports*, 10(10):1646–1654, 2015.
- [4] Coen Honingh. Towards a symmetry breaking model of a sea anemone through reaction-diffusion systems. Master’s thesis, University of Amsterdam, Computational Science Lab, 2020.
- [5] Steven Oud. Symmetry breaking gene regulatory networks in *nematostella vectensis*. University of Amsterdam, Computational Science Lab, 2022.
- [6] Koen Greuell. Spatial expression profiles of developmental regulatory genes compared to a computational model of directive axis formation in the sea anemone *nematostella vectensis*. Master’s thesis, University of Amsterdam, Computational Science Lab, 2020.
- [7] Yves Fomekong-Nanfack, Jaap A Kaandorp, and Joke Blom. Efficient parameter estimation for spatio-temporal models of pattern formation: case study of *drosophila melanogaster*. *Bioinformatics*, 23(24):3356–3363, 2007.
- [8] Gerald M Rubin. *Drosophila melanogaster* as an experimental organism. *Science*, 240(4858):1453–1459, 1988.
- [9] Mark D Adams, Susan E Celniker, Robert A Holt, Cheryl A Evans, Jeannine D Gocayne, Peter G Amanatides, Steven E Scherer, Peter W Li, Roger A Hoskins, Richard F Galle, et al. The genome sequence of *drosophila melanogaster*. *Science*, 287(5461):2185–2195, 2000.

- [10] Claus Nielsen. Six major steps in animal evolution: are we derived sponge larvae? *Evolution & development*, 10(2):241–257, 2008.
- [11] John R Finnerty, Kevin Pang, Pat Burton, Dave Paulson, and Mark Q Martindale. Origins of bilateral symmetry: Hox and dpp expression in a sea anemone. *Science*, 304(5675):1335–1337, 2004.
- [12] Michael J Layden, Fabian Rentzsch, and Eric Röttinger. The rise of the starlet sea anemone *nematostella vectensis* as a model system to investigate development and regeneration. *Wiley Interdisciplinary Reviews: Developmental Biology*, 5(4):408–428, 2016.
- [13] Nicholas H Putnam, Mansi Srivastava, Uffe Hellsten, Bill Dirks, Jarrod Chapman, Asaf Salamov, Astrid Terry, Harris Shapiro, Erika Lindquist, Vladimir V Kapitonov, et al. Sea anemone genome reveals ancestral eumetazoan gene repertoire and genomic organization. *science*, 317(5834):86–94, 2007.
- [14] Grigory Genikhovich and Ulrich Technau. On the evolution of bilaterality. *Development*, 144(19):3392–3404, 2017.
- [15] Fabian Rentzsch, Roman Anton, Michael Saina, Matthias Hammerschmidt, Thomas W Holstein, and Ulrich Technau. Asymmetric expression of the bmp antagonists chordin and gremlin in the sea anemone *nematostella vectensis*: implications for the evolution of axial patterning. *Developmental biology*, 296(2):375–387, 2006.
- [16] Michael Saina, Grigory Genikhovich, Eduard Renfer, and Ulrich Technau. Bmps and chordin regulate patterning of the directive axis in a sea anemone. *Proceedings of the National Academy of Sciences*, 106(44):18592–18597, 2009.
- [17] Rudolf Gesztelyi, Judit Zsuga, Adam Kemeny-Beke, Balazs Varga, Bela Juhasz, and Arpad Tosaki. The hill equation and the origin of quantitative pharmacology. *Archive for history of exact sciences*, 66:427–438, 2012.
- [18] Claudia Mieko Mizutani, Qing Nie, Frederic YM Wan, Yong-Tao Zhang, Peter Vilmos, Rui Sousa-Neves, Ethan Bier, J Lawrence Marsh, and Arthur D Lander. Formation of the bmp activity gradient in the drosophila embryo. *Developmental cell*, 8(6):915–924, 2005.
- [19] Lawrence J Fogel, Alvin J Owens, and Michael J Walsh. Intelligent decision making through a simulation of evolution. *Behavioral science*, 11(4):253–272, 1966.
- [20] COMSOL. Multiphysics<sup>®</sup> v. 6.1. [www.comsol.com](http://www.comsol.com), 2022. Stockholm, Sweden.
- [21] Uri M Ascher and Linda R Petzold. *Computer methods for ordinary differential equations and differential-algebraic equations*, volume 61. Siam, 1998.

- [22] Thomas Philip Runarsson and Xin Yao. Search biases in constrained evolutionary optimization. *IEEE Transactions on Systems, Man, and Cybernetics, Part C (Applications and Reviews)*, 35(2):233–243, 2005.
- [23] John A Nelder and Roger Mead. A simplex method for function minimization. *The computer journal*, 7(4):308–313, 1965.
- [24] Pauli Virtanen, Ralf Gommers, Travis E. Oliphant, Matt Haberland, Tyler Reddy, David Cournapeau, Evgeni Burovski, Pearu Peterson, Warren Weckesser, Jonathan Bright, Stéfan J. van der Walt, Matthew Brett, Joshua Wilson, K. Jarrod Millman, Nikolay Mayorov, Andrew R. J. Nelson, Eric Jones, Robert Kern, Eric Larson, C J Carey, İlhan Polat, Yu Feng, Eric W. Moore, Jake VanderPlas, Denis Laxalde, Josef Perktold, Robert Cimrman, Ian Henriksen, E. A. Quintero, Charles R. Harris, Anne M. Archibald, Antônio H. Ribeiro, Fabian Pedregosa, Paul van Mulbregt, and SciPy 1.0 Contributors. SciPy 1.0: Fundamental Algorithms for Scientific Computing in Python. *Nature Methods*, 17:261–272, 2020. doi: 10.1038/s41592-019-0686-2.